Institut für Veterinärpharmakologie und –toxikologie
der Vetsuisse-Fakultät Universität Zürich

Direktor: Prof. Dr. med. vet. Felix R. Althaus

Arbeit unter wissenschaftlicher Betreuung von
PD Dr. rer. nat. Sascha Beneke

PARP Activity in Cancer Cell Lines

Inaugural-Dissertation

Zur Erlangung der Doktorwürde der
Vetsuisse-Fakultät Universität Zürich

vorgelegt von

Jennifer Brandenburg

Tierärztin
von Deutschland

genehmigt auf Antrag von

Prof. Dr. med. vet. Felix R. Althaus, Referent
PD Dr. med. vet. Carla Rohrer Bley, Korreferentin

2014

Table of Contents

1. Zusammenfassung

Die Familie der Poly(ADP-Ribose)Polymerasen besteht aus 17 Enzymen, von denen allerdings nur sechs in der Lage sind, ein Polymer aus (ADP-Ribose)-Ketten (PAR) zu synthetisieren. Die restlichen Mitglieder besitzen mehrheitlich Mono(ADP-Ribose)-Transferase-Aktivität oder sind inaktiv. Das Enzym PARP1, welches für bis zu 90% der PAR-Produktion nach DNA-Schädigung verantwortlich ist, ist der wohl prominenteste Vertreter dieser Familie. Die Synthese von PAR ist wichtig für unterschiedliche zelluläre Prozesse, u.a. in Transkription, Replikation, Epigenetik, Entzündungsreaktionen, Zelltod und Signalisierung von DNA-Schäden. PARP1 ist insbesondere beteiligt an der Reparatur von DNA-Einzelstrangbrüchen, weswegen PARP-Inhibitoren in der Onkologie auf Versuchsbasis eingesetzt werden. In der Krebstherapie finden diese Inhibitoren entweder als Monotherapie oder aber in Kombination mit verschiedenen Chemotherapeutika bzw. ionisierender Strahlung Anwendung. Der Einsatz von PARP-Inhibitoren als alleiniges therapeutisches Mittel setzt einen Defekt in der Homologen Rekombination voraus, beispielsweise in den BRCA1/2 –Proteinen, wie es in bestimmten Krebsarten der Fall ist. Die Zellen sind somit unfähig, DNA-Doppelstrangbrüche zu reparieren. PARP-Inhibitoren erhöhen die Rate an Einzelstrangbrüchen, die bei der Replikation in letale Doppelstrangbrüche konvertiert werden. Im Fall einer kombinierten Therapie wird die DNA-schädigende Wirkung des eingesetzten Agens durch PARP-Inhibitoren verstärkt, was zur Dosisreduktion des Genotoxins genutzt werden kann. Allerdings gilt es zu beachten, dass PARP1 multiple Funktionen in der Zelle erfüllt, wobei man zwischen (essentieller) basaler Aktivität und DNA-Schaden-stimulierter Aktivität unterscheiden muss. Die Polymere der basalen Aktivität sind kurz, und die Synthese wird nur durch relativ hohe Dosen der kompetitiv-wirkenden PARP-Inhibitoren gehemmt. Hingegen sind Strangbruch-induzierte Polymere lang, was die Synthese sensitiver für selbst geringere Inhibitor-Konzentrationen macht. Um die basale Aktivität möglichst wenig zu beeinträchtigen, sollten geringe, angepasste Dosen der PARP-Inhibitoren verwendet werde.

In der vorliegenden Arbeit sollte nun untersucht werden, ob sich die PAR-Syntheseleistung (Kapazität) in verschiedenen Tumorzelllinien unterscheidet und ob die Zellen unterschiedlich sensitiv auf PARP-Inhibitoren reagieren (Plastizität). Um PAR-Spiegel in Zelllysaten bzw. intakten Zellen zu messen, wurde eine einfache, schnell durchzuführende Methode etabliert. Mit diesem Protokoll wurden Standard-Parameter der Enzymologie wie Affinität zum Substrat NAD^+ (K_M) und maximale Reaktionsgeschwindigkeit (V_{max}) der PARP-Aktivität in den Zelllysaten bestimmt. Die Ergebnisse wiesen signifikante Unterschiede für V_{max} auf, während K_M für alle Zelllinien gleich war. Nachfolgend wurden intakte Zellen mit dem DNA-schädigenden Agens Wasserstoffperoxid als etabliertem Aktivator der PARP1 behandelt und die PAR-Kapazität bestimmt. Anschließend wurde bei einer geringen und einer hohen H_2O_2-Dosis die Plastizität der Reaktion bei PARP-Inhibition bestimmt. Es zeigte sich, dass sowohl die Kapazität als auch die Plastizität sehr spezifisch für die betrachtete Zelllinie sind. Dies korreliert weder mit der Konzentration an vorhandenem PARP1 Protein noch mit dem Level der vorhandenen basalen Poly(ADP-Ribose). Schlussendlich wurde die Viabilität der unterschiedlichen Tumorzelllinien nach

Toxin-Behandlung mit oder ohne PARP-Inhibitor bestimmt. Hierbei wurden H_2O_2 und das Chemotherapeutikum Temozolomid verwendet. Es konnte nachgewiesen werden, dass die Reduktion der Viabilität nach DNA-Schädigung nicht nur unterschiedlich zwischen den Tumorzelllinien ist, sondern auch stark durch das entsprechende Toxin bestimmt wird. Zusätzlich ist der Einfluss des PARP-Inhibitors auf die Viabilität nicht nur von diesen beiden Parametern abhängig, sondern auch von der applizierten Dosis des Genotoxins. Bei geringen Konzentrationen sensitiviert die PARP-Inhibition manche Tumorzellen, bei hohen Dosen wirkt es in der Regel protektiv. Letzteres lässt sich darauf zurückführen, dass Überaktivierung der PARP1 durch DNA-Strangbrüche zu einer NAD^+-Depletion und damit zum Zelltod führt.
Zusammenfassend kann gesagt werden, dass grundlegende Unterschiede in PARP-Aktivitätsparametern zwischen verschiedenen Krebszelllinien festgestellt wurden. Dies unterstreicht die Notwendigkeit, jeden Tumortyp einzeln bezüglich seiner Sensitivität auf ein Chemotherapeutikum sowie auf eine Kombination dessen mit einem PARP-Inhibitor zu evaluieren, um die bestmögliche Therapieform für jedes Individuum festlegen zu können.

2. Abstract

PARP1 is the most abundant and active member of the poly(ADP-ribose)polymerase (PARP) family of ADP-ribose transferases, responsible for about 90% of poly(ADP-ribose) (PAR) synthesis after DNA damage. PARP1 has been shown to play a role in transcription, replication, epigenetics, DNA damage signaling, inflammation and cell death. Its involvement in DNA repair processes makes it an attractive target in oncology. PARP inhibitors as accessory pharmaceuticals enhance the efficacy of chemotherapeutics by diminishing repair of DNA single strand breaks and have been under investigation since the 90´s of the last century. Cancer treatment with PARP inhibitors as monotherapy is an emerging field of research and phase-III clinical trials are currently ongoing. This approach makes use of the fact that cancers mutated in homologous recombination proteins BRCA1/ 2 are unable to repair DNA double strand breaks, which arise during replication from persistent nicks and gaps induced by abrogated PARP1 activity. But as PARP1 has many roles in cell homeostasis, reducing inhibitor concentration to a minimum should be a major goal in personalized medicine.

The aim of the thesis was to investigate if total PAR production (capacity) differs between cancer cell lines and whether they also respond differently to PARP inhibition (plasticity).

First, a standardized protocol was developed to measure PARP1 levels and total PARP activity in cancer cell lysates for analysis of PAR forming capacity. Results showed broad distribution in PARP1 levels. Enzyme kinetics from activity assays revealed equal substrate affinities (Michaelis-Menten constant K_M) but significant variation in reaction velocities (V_{max}) for the different cancer cell lines. In the next step, cells were challenged with H_2O_2 alone or including the PARP inhibitor PJ-34. Deduced from this data, the capacity and plasticity of PARP1 reactions in intact cells were determined, the latter indicating the responsiveness to increasing inhibitor concentration. Both parameters, capacity and plasticity, were found to be very specific for each cell line, correlating neither with PARP1 amount nor with basal PAR level. Finally, to support the *in vitro* data, viability assays were conducted with H_2O_2 or temozolomide, each alone and in combination with PJ-34 to analyze viability of cancer cell lines after cytotoxic challenge. It could be demonstrated that cell response was dependent on the combination of cell line, cytotoxic agent and PARP inhibitor. While at lower dosages PJ-34 sensitized some cell lines to the cytotoxic agent, a protective effect was observed in some cases at high concentrations, probably due to the preservation of NAD^+ by abrogated PARP activity, reducing cell death by energy depletion

In summary, the experiments revealed substantial differences of cancer cell lines in PARP1 levels, as well as activity parameters such as capacity and plasticity. PARP1 expression, plasticity and sensitivity towards genotoxic agents did not correlate with each other, emphasizing the need to evaluate the sensitivity of each type of cancer in combination with the respective chemotherapeutic agent to PARP inhibition.

3. Abbreviations

Abbreviation

APS	Ammonium persulfate
bp	Base pairs
BSA	Bovine serum albumin
CHAPS	3-[(3-cholamidopropyl)dimethylammonio]-1-propanesulfonate
ddH_2O	Double-distilled water
DMEM	Dulbecco's modified Eagle's Medium
DMSO	Dimethyl sulfoxide
DNase	Deoxyribonuclease
dsDNA	Double-stranded DNA
DTT	1,4-Dithiothreitol
EDTA	Ethylenediamine-tetraacetic acid
FCS	Fetal calf serum
HEPES	N-(2-hydroxyethyl)-piperazine-N'-2-ethanesulfonic acid
HR	Homologous recombination
kDa	Kilo Dalton
K_M	Michaelis-Menten value
LPSC	Lysis Protocol Sf-9 Cells
M	Marker
NAD^+	Nicotinamide adenine dinucleotide
NP40	Nonidet P40
PAR	Poly(ADP-ribose)
PARG	Poly(ADP-ribose)glycohydrolase
PARP	Poly(ADP-ribose)polymerase
PBS	Phosphate-buffered saline
Pen/Strepto	Penicillin/ Streptomycin
PMSF	Phenylmethylsulphonylfluoride
RIPA	Radioimmunoprecipitation assay
rpm	Rotations per minute
SD	Standard deviation
SDS	Sodiumdodecylsulfate
SEM	Standard error of the mean
TAE	Tris acetic acid EDTA buffer
TCA	Trichloroacetic acid
TEMED	N,N,N´,N´-Tetramethylethylenediamine
TMZ	Temozolomide
TNT	Tris-NaCl-Tween 20
V_{max}	Maximum reaction velocity
β-MeEtOH	β-Mercaptoethanol

4. Introduction

PARP in general

The family of poly(ADP-ribose)polymerases (PARPs) consists of 17 members. While most of them are limited to mono(ADP-ribosyl)ation, six are true polymerases (Rouleau et al., 2010). For two members enzymatic activity remains undetermined (Hottiger et al., 2010).

With localizations ranging from nucleus to cytoplasm depending on each PARP (Smith, 2001), the enzymes are suspected to have a variety of important but independent functions. The most abundant family member, PARP1, has been shown to be involved in inflammation (Review Beneke et al, 2004, Beneke 2008), cell death, transcription, and DNA repair (Review Mangerich & Bürkle, 2011). The latter one is the most prominent and has been described first.

Using NAD^+ as substrate, PARP1 synthesizes ADP-ribose by cleaving off nicotinamide and linking two ADP-ribose units by a glycosidic bond (Diefenbach & Bürkle, 2005). This reaction is repeatable and a long and branched polymer can be formed. PARP1 has been shown to act as a dimer with two NAD^+ molecules necessary as substrate (Alvarez-Gonzalez and Mendoza-Alvarez, 1995). Synthesis of poly(ADP-ribose) (PAR) can be divided into three steps: initiation (attaching the first ADP-ribose unit), elongation (chain extension) and branching (addition of side chains) (Alvarez-Gonzalez and Mendoza-Alvarez, 1995). PAR chains can consist of up to 200 ADP-ribose units in linear arrangement with multiple branching points (Review Diefenbach & Bürkle, 2005). PAR can be covalently attached to a variety of proteins, modifying their activity through its negative charge (Smith, 2001). The most important acceptor protein is PARP1 itself. Of note, many proteins can also bind to PAR chains in a non-covalent fashion. The strongest activator stimulus for PARP1 is its binding to DNA breaks and aberrant DNA structures (Potaman et al., 2005).

In cases of single strand DNA breaks, PARP1 is localizing to the site of damage within seconds, starting PAR production and thus leading to a recruitment of different proteins, among others XRCC1, a polypeptide important in base excision repair (BER) pathway (El-Khamisy et al., 2003). Besides BER, PARP1 also plays a role in the nucleotide excision repair (NER) and it was shown that abrogated PARP1 activity delays both BER and NER (Flohr et al., 2003). Apart from single strand repair, PARP1 has been shown to influence DNA double strand break repair mechanisms. Ruscetti et al. (1998) demonstrated the interaction of PARP1 with the DNA-dependent protein kinase, an enzyme involved in non-homologous end joining, whereas Haince et al. (2007, 2008) identified PARP1 to be responsible for recruiting and activating protein complexes and kinases crucial for sensing double strand breaks and initiating homologous recombination pathways.

PARP activity differs considerably among gender and species. In humans, men display a twofold higher activity compared to women (Zaremba et al., 2011). Interspecies variation correlates to differences in life span: human peripheral blood mononuclear cells have a five times higher activity compared to those of short-lived rats (Grube & Bürkle, 1992), which depends solely on the amino acid composition (Beneke et al., 2010).

Contrary to normal cells, cancer cells often show increased PARP activities. Level of poly(ADP- ribosyl)ation in human hepatocellular carcinomas was found to be

twice as high as in liver cirrhosis, and about 14 times higher than in normal liver cells (Shiobara et al., 2001). Also, PARP activity of lymphocytic leukemia cells (L1210) was four times greater than that of normal human peripheral blood lymphocytes (Plummer et al., 2005). However, it is essential to distinguish PARP activity from expression: in a human population Zaremba et al. (2011) showed a wide range of PARP activity in peripheral blood mononuclear cells with a narrow spectrum in expression. Stimulateable PARP activity in a cell is determined by four parameters: PARP1 protein amount, rate of pre-modification, allele type and regulating partners (Krukenberg et al., 2014).

Influence of allele variation on PARP1 activity is demonstrated by the Single Nucleotide Polymorphism at position 762. One T to C base transition results in an amino acid exchange of valine to alanine, resulting in reduced activity (Lockett et al., 2004). The alanine variant displays a 50 % drop in activity (Wang et al., 2007), due to reduced reaction velocity with unaltered substrate affinity (Beneke et al., 2010). Allele frequency varies between ethnic groups. Americans with European descent have an alanine-allele frequency of only 19 % whereas those of African descent only hold the C allele by 0 (Lockett et al., 2004; Smith et al., 2008) to 5 %. (Gao et al., 2008).

By comparing different cancer cells Zaremba et al. (2009) found a 3.5 fold variation in PARP1 amount and in contrast to normal cells, cancer cells even displayed a 23 times higher PARP1 level. So far Ewing sarcoma cells displayed the highest protein and activity levels (Soldatenkov et al., 1999).

There is a constitutive low level of PAR in every cell (Fiorillo et al., 2006, Martello et al., 2013). Among others, basic PARP activities play a role in transcription, replication und telomere-length (Ji & Tulin, 2010; Beneke et al., 2008; Gibson & Kraus, 2012). While PAR formed upon DNA damage is degraded within seconds to minutes, constitutive PAR has a half time of hours (Alvarez-Gonzalez & Althaus, 1989). Additionally, inhibition of basic PAR formation requires higher inhibitor concentrations than DNA damage induced PAR production (Martello et al., 2013). High basic PAR levels are supposedly correlated with a high degree of PARP1 modification. Automodification reduces enzymatic activity of PARP1 with every attached ADP-ribose unit (Kawaichi et al., 1981).

PARP inhibitors in cancer therapy

Its role in DNA repair makes PARP1 an interesting target in oncology.

The poly(ADP-ribosyl)ation reaction after activation by binding to DNA breaks recruits DNA-repair enzymes (He et al., 2010). Thus, PARP1 activity facilitates proper repair, suggesting a correlation between cancer formation and low PARP1 activity, which indeed has been reported (Lockett et al., 2004; Figueroa et al., 2007; Chiang et al., 2008).

Without PARP1 DNA single strand breaks sustain and are turned into double strand breaks during the next replication. Double strand breaks are repaired during S-phase and G2 by the homologous recombination (HR) and cells are able to recover (He et al., 2010). However, if cells are incapable of performing HR (e.g. BRCA1 and BRCA2 negative cancer cells) breaks persist and eventually cause cell death. Consequently, in this specific case the inhibition of PARP1 as single treatment is exploited in cancer therapy trials.

Efficacy of genotoxic chemotherapeutics can be also enhanced by application of PARP1 inhibitors. High extent of DNA damage together with abrogated PARP1

activity leads to massive accumulation of single strand breaks, exhausting DNA repair capacity and driving cells into apoptosis (He et al., 2010). So far, PARP1 inhibitors are combined with alkylating agents, topoisomerase I inhibitors or ionizing radiation (Mangerich & Bürkle, 2011).

All reported PARP inhibitors compete with NAD^+ for binding to the catalytic cleft (Cepeda et al., 2006) and inhibition is fully reversible. First generation inhibitors targeted all PARPs unspecifically (Review Bürkle, 2001), but newly developed inhibitors are already more selective towards specific PARP family members (Ekblad et al., 2013). Currently a great number of clinical trials are ongoing, testing effects of PARP inhibitors such as Olaparib (AZD2281), BSI-201 or Veliparib (ABT-888) on all types of cancers like prostate-, lung-, ovarian-, breast cancer etc. (www.clinicaltrials.gov).

PJ-34 is another potent PARP inhibitor first synthetized by Soriano et al. in 2001, with the advantage of a high degree of water solubility. A vast number of experiments with various cancer cell lines in culture have already been published using PJ-34 alone or in combined treatments. Huang et al. (2008) showed liver carcinoma cells to increasingly go into apoptosis when treated with PJ-34; as did some lung cancer cell lines (Gangopadhyay et al., 2011) without impairing viability of normal cells. In liver cancers, PJ-34 additionally increased efficacy of DNA damaging drugs (Huang et al., 2008). Similar results were shown for basal-like breast cancer cells, with cells already sensitive to PJ-34 treatment alone (Hastak et al., 2010).

In this thesis, PJ-34 was combined with the cytotoxic agents H_2O_2 and temozolomide, a chemotherapy-drug used in the clinic to treat malignant gliomas or anaplastic astrozytomas due to its ability to penetrate the blood-brain-barrier (www.cancer.gov). Several studies have been conducted testing temozolomide in combination with PARP inhibitors, i.e. NU1025 and NU1085 (Delaney et al., 2000). Both inhibitors were able to increase the cytotoxicity of temozolomide in all tested cell lines.

Plummer et al. (2008) demonstrated a reduction of temozolomide's toxic dosage from 250 to 200 mg/m^2 in patients also receiving the PARP inhibitor AG014699, with AG014699 alone displaying no side effects at effective concentrations.

PARP1 activity can be divided into two different levels: basic low-level activity producing localized short and persistent polymer needed for cellular maintenance (transcription, telomere regulation), as well as high-level synthesis with long, branched but short-lived PAR, enabling quick chromatin remodeling to facilitate repair. As inhibitors are competitive, abrogating the formation of long PAR (i.e. repair) is achieved at lower doses as the suppression of synthesis of short PAR (i.e. transcription). To minimize potential side-effects arising from targeting basic PARP1 activity, it would be reasonable to reduce inhibitor concentration in such a way that only damage-related PARylation is suppressed.

Objectives

Objective of this dissertation was the development of an easy, standardized protocol to measure total PARP1 activity (capacity) in cancer cells. The resulting data were correlated to (I) PARP1 protein levels, (II) applied dose and (III) nature of genotoxin, as well as (IV) the responsiveness to PARP inhibition (plasticity). For this, different cancer cell lines were challenged with cytotoxic agents including hydrogen peroxide as classical PARP1 activator and the chemotherapeutic drug temozolomide. In parallel, the PARP inhibitor PJ-34 was used to define the respective minimum inhibitor concentrations which block PAR synthesis in these cells. To cover a wide spectrum of different cancer cell types, the following five cancer cell lines were chosen for the assays: HeLa (cervical cancer), HepG2 (hepatocellular carcinoma), MCF-7 (breast cancer), SH-SY5Y (neuroblastoma) and U2OS (osteosarcoma).

As PARP1 has many roles in cell homeostasis, reducing inhibitor concentration to a minimum is fundamental. Goal is to underline the importance of treating each cancer patient individually, thus making a step towards personalized medicine.

5. Material

If not stated otherwise, chemicals are solved and diluted in ddH_2O.

Chemicals	*Company*
NP40	AppliChem
2-Propanol	Sigma
Acetic acid	Merck KGaA
Acrylamide 4K (40 %)	AppliChem
Acrylamide Solution (40 %) Mix 19:1	AppliChem
Agarose low EEO	AppliChem
APS	AppliChem
Bromphenol Blue Sodium Salt	AppliChem
BSA Fraction V	GE Healthcare
$CaCl_2$	Fluka
CHAPS	Sigma
Chloroform: Isoamylalcohol	Sigma
DMEM Glutamax	Life Technologies
DMSO	Sigma
DNase I	AppliChem
DTT	AppliChem
EDTA	AppliChem
Ethanol	Fluka
Ethidium Bromide	Sigma
FCS (heat inactivated)	Life Technologies
Formamid	Fluka
Glucose	Sigma
Glycerol 100 %	AppliChem
Glycin	Applichem
HCl 32 %	Merck
HEPES	Life Technologies
KH_2PO_4 (Potassium phosphate monobasic)	Sigma
KOH	Fluka
Methanol	Fluka
$MgCl_2$	Fluka
Na_2HPO_4	Sigma-Aldrich
NaCl	AppliChem
NAD^+ >/=95 % HPLC	Biochemika
Pen/Strepto	Life Technologies
Phenol	Sigma
PMSF	Fluka
Protamine sulfate	Sigma
Protease Inhibitor Cocktail Complete EDTA free	Roche Diagnostics GmbH
Proteinase K	Fermentas

Rapilait (milk)	Bio RAD
Resazurin	Alfa Aesar
RPMI	Life Technologies
SDS	Sigma
Sodium deoxycholate	Sigma
SuperSignal West Femto Maximum Sensitivity Substrate	Thermo Scientific
TCA	Fluka
TEMED	AppliChem
Temozolomide	Sigma-Aldrich
Tris	AppliChem
Trypsin 2,5%	Life Technologies
Tween 20	Fluka
Urea	AppliChem
β-Mercaptoethanol	Life Technologies

6. Methods

6.1. Cell Culture

For composition of culture media of different cancer cell lines see Table 1. All cells were kept at 37 °C and 5 % CO_2 in a Hera Cell 240 incubator (Heraeus) and were split twice a week under a sterile hood. Prior to splitting all solutions were pre-warmed to 37 °C. After microscopic control old medium was discarded. Cell layer was washed with PBS (137 mM NaCl, 8 mM Na_2HPO_4, 2.7 mM KCl, 0.9 mM KH_2PO_4) to further remove dead cells and old medium. For detachment of cells trypsin (Life Technologies) was added and cells were incubated for 5 minutes at 37 °C before being washed off the plate with new medium. For culturing cells were transferred 1: 5 onto new dishes. Cell counts were determined with a TC10 Automated Cell Counter (Bio-Rad) before cell suspension was centrifuged and the pellet taken for experiments.

Media	DMEM GlutaMAX	DMEM	DMEM/ RPMI (1:2)
Additives	+ 10 % FCS + 1 % Pen/Strepto	+ 10 % FCS + 1 % Pen/Strepto	+ 10 % FCS + 1 % Pen/Strepto
Cells	HeLa (cervical cancer) MCF-7 (breast cancer)	U2OS (osteosarcoma) HepG2 (hepatocellular carcinoma)	SH-SY5Y (neuroblastoma)

Table 1: Media and additives for different cancer cells.

6.2. Synthesis of PAR Standard

PAR Standard is needed in slot blotting and was synthesized according to Fahrer et al. (2007). A 10 ml reaction mix was prepared (100 mM Tris HCl pH 7.5, 10 mM $MgCl_2$, 1 mM DTT, 50 µg/ ml dsDNA activator oligonucleotide (GGAATTCC), 1 mM NAD^+, 75 nM human PARP1 (C908G by Sascha Beneke)). During 20 minutes PAR was synthesized at 37 °C. Reaction was stopped with one volume of 20 % ice cold TCA and mix was left on ice for another 15 minutes. After being aliquoted into 2 ml samples and centrifuged at 9000 x g for 10 minutes at 4 °C, supernatants were removed. Pellets were washed twice in ethanol (-20 °C), each washing followed by centrifugation as above. Afterwards pellets were air-dried.
For protein digestion, each pellet was resuspended in 900 µl KOH (0.5 M) / EDTA (50 mM), incubated for 10 minutes at 37 °C and 100 µl Tris HCl (1 M, pH 8.0) was added. Samples were poured together again and the pH was modified to 7.5 with HCl (32 %). Aliquoted again into 2 ml, samples received 25 µl $MgCl_2$ (2 M) and 55 µl DNase I (2 mg/ ml, AppliChem) each and were left in a Thermomixer Comfort 35680 (Vaudaux-Eppendorf AG) at 37 °C and 600 rpm. After two hours 10 µl $CaCl_2$ (100 mM) and 11 µl Proteinase K (20 mg/ ml, Fermentas) were added to each fraction and overnight incubation followed.
The next day DNA and proteins were extracted as follows: each sample was mixed with 600 µl phenol and centrifuged at 14,000 x g for 10 minutes at room temperature. Aqueous supernatants were taken into new tubes to repeat previous extraction step with 600 µl chloroform:isoamylalcohol (24:1). Finally

aqueous supernatants were pooled and filled up with 100 % ethanol (-20 °C) to an end concentration of 70 % for overnight ethanol precipitation at -20 °C.
Next day, sample was centrifuged at 9000 x g for 30 minutes at 4 °C, pellet was air dried and solved in water. PAR concentration was determined photometrically with NanoDrop 2000c (Thermo Scientific). Sample was measured at 260 nm and PAR concentration was calculated according to the Lambert-Beer law.

LAMBERT-BEER: $E_\lambda = \varepsilon_\lambda \cdot c \cdot d$ corresponding to $c = E_\lambda : (\varepsilon_\lambda \cdot d)$

with E_λ as extinction (= measured value), ε_λ as extinction coefficient for mono(ADP-ribose) (= 13.500 $M^{-1}\,cm^{-1)}$ and d as diameter (= 1 cm).

6.3. Development of a Suitable Lysis Protocol

For PARP1 extraction from mammalian cells different protocols were compared: LPSC (Lysis Protocol Sf-9 Cells, Beneke et al., 2000), CHAPS-buffer based and RIPA-buffer based lysis protocols. LPSC comprised a centrifugation step with Protamine sulfate (Sigma) and as additional measure, CHAPS and RIPA protocols were modified with higher NaCl concentrations and Protamine sulfate supplement and included in comparison. Criteria were high PARP1 yield with complete extraction of PARP1 from chromatin and preservation of enzymatic activity. CHAPS and RIPA are standard protocols for mammalian cell lysis whereas LPSC is normally used for Sf-9 insect cells. For compositions of lysis buffers see Table 2.

	LPSC	CHAPS	RIPA
Lysis Buffer	25 mM Tris HCl pH 8.0 50 mM Glucose 10 mM EDTA pH 8.0 1 mM PMSF 1 mM β-MeEtOH 0.2 % Nonidet P40 0.2 % Tween 20 500 mM NaCl	10 mM TrisHCl pH 7.5 100 mM NaCl 20 % Glycerol 0.5 mM PMSF 5 mM β-MeEtOH different urea concentrations 1 mM MgCl2 1 % CHAPS 1x Protease Inhibitor Cocktail 500 mM NaCl	25 mM Tris HCl pH 7.5 150 mM NaCl 1 % Sodium deoxycholate 1 mM PMSF 0.1 % SDS 1 % Nonidet P40 500 mM NaCl
added after first centrifugation	1 mg/ml Protamine sulfate	1 mg/ml Protamine sulfate	1 mg/ml Protamine sulfate

Table 2: Contents of the five lysis buffers LPSC, CHAPS, RIPA, modified CHAPS and modified RIPA. Urea concentrations in CHAPS protocol varied from 0-1 M. Blue boxes indicate modifications of protocols. Modified CHAPS was conducted without urea. PMSF was solved in ethanol.

6.3.1. Cell Lysis

For comparison of lysis protocols, HeLa cells were used as starting material.

After harvesting, cells were centrifuged at 2500 x g for 5 minutes at room temperature, washed in ice cold PBS and centrifuged at 2500 x g for 5 minutes at 4 °C. Subsequent steps were done on ice or at 4 °C. The respective lysis buffer was added to the cell pellet. Suspensions were incubated on a Rotator SB2 (Stuart) before centrifuging (different settings for respective lysis protocols, see Table 3 for details). For LPSC and modified versions of CHAPS and RIPA, supernatant 1 was transferred into new tube and Protamine sulfate (in water) pre-warmed to 40 °C was added 1 mg/ml to precipitate DNA. Sample was centrifuged a second time at 16,100 x g and supernatant 2 was used for further experiments.

	Incubation	1st Centrifugation	2nd Centrifugation
LPSC	20 min	16,100 x g / 20 min	16,100 x g / 10 min
CHAPS	30 min	16,100 x g / 30 min	-
Modified CHAPS	30 min	16,100 x g / 30 min	16,100 x g / 10 min
RIPA	15 min	14,000 x g / 15 min	-
Modified RIPA	15 min	16,100 x g / 30 min	16,100 x g / 10 min

Table 3: Settings for the different lysis protocols.

6.3.2. Dialysis

In cases where dialysis was performed, Slide-A-Lyzer Dialysis Cassettes, MWCO 20,000 (Thermo Scientific) were used in an overnight step. Supernatants 2 were dialyzed against 20 % glycerol/ PBS at 4 °C to stabilize the proteins in aqueous solution and to remove detergents and other small contaminants. The dialysis buffer was taken as reference for protein measurements. Samples were frozen in liquid nitrogen and stored at -80 °C until further needed.

6.3.3. Protein Measurement

Protein measurements were performed with NanoDrop 2000c Spectrophotometer and the computer program NanoDrop 2000/ 2000c (Thermo Scientific). A dilution series of 1, 0.5, 0.2, 0.1 and 0 of each sample was made with the respective reference buffer. UV-Vis settings were selected and dilution series were measured against their reference buffer at 235 nm and 280 nm according to Whitaker and Granum (1980), without baseline correction. Deionized water was used in between samples as blank. From each dilution triplicates were measured and obtained values were analyzed with Excel and Graph Pad Prism 6. From the results of 235 nm those of 280 nm were subtracted and thereof the mean for each triplicate was calculated. Steepness of the slope was determined by linear regression analysis. To receive total protein amount in µg/ µl, slope was divided by 2.51 (Whitaker & Granum, 1980) and multiplied by 10 to compensate for an absorbance of 1 mm in UV-Vis settings when standard for other settings is 10 mm.

6.4. Agarose Gels

To perform PARP activity assays as controlled as possible, it is beneficial to remove any remaining genomic DNA in samples. Residual DNA could activate PARP1 and possibly affect activity assay results.
Agarose gels were performed to check for remaining DNA. Starting with different amounts of lysis buffer, loaded sample volumes corresponded to about $3.7 \cdot 10^4$ cells (except for LPSC with $9.4 \cdot 10^4$ cells). For RIPA lysis, the first pellet was resuspended in 500 µl PBS and 7.5 µl were used for agarose gel.
Prior to loading, 6x DCD Loading Buffer (Fermentas) was added to samples and Mass Ruler DNA Ladder Mix (Fermentas) was applied as marker. A 0.8 % agarose (low EEO) gel was run in TAE (40 mM Tris HCl pH 8.0, 20 mM acetic acid, 1 mM EDTA) at 80 - 100 Volts. Afterwards gel was incubated for 15 minutes in ethidium bromide at room temperature and on slow shaker before excess ethidium bromide was washed out with deionized water for 10 minutes. Image Lab 4.1 and Intelligent Dark Box (Fujifilm) were used for picture acquisition.

6.5. Western Blotting

For PARP1 levels in different cancer cells and comparison of PARP1 and PAR amounts after different lysis protocols, Western blots were carried out. All materials were supplied by Bio-Rad. Separating and stacking gels were prepared as seen in Table 4.

	Separating Gel (10 %)	Stacking Gel (3 %)
Buffer	1260 µl	620 µl
SDS 10 %	105 µl	50 µl
Acrylamide 40 %	2600 µl	375 µl
TEMED	21 µl	25 µl
APS 10 %	53 µl	50 µl
ddH_2O	6430 µl	3925 µl

Table 4: Composition of separating and stacking gel.

Separating buffer (3 M Tris pH 8.9) and stacking buffer (500 mM Tris pH 6.7) were used for separation and stacking gel, respectively. After pouring separation gel a fine layer of 2-propanol was loaded on top to straighten gel surface. Gels were left to polymerize for a minimum of 30 minutes. 2-propanol was discarded and residues were eliminated by absorption with Whatman paper. Stacking gel was poured and inserted with a suitable comb, gel was left to polymerize for another 30 minutes. Gel electrophoresis unit was put together and filled with SDS-PAGE buffer (25 mM Tris pH 8.6, 0.192 M glycin, 0.1 % SDS). Prior to loading, samples were mixed with 5 x Loading Dye (284.1 mM Tris HCl pH 6.8, 4.55 % SDS, 22.73 % glycerol, 325 mM β-MeEtOH, bromphenol blue), heated up to 95 °C for 5 minutes and centrifuged at full speed for 10 seconds. PageRuler Prestained Protein Ladder (Thermo Scientific) was loaded as marker. Gels were run at 11 mA per gel until samples had moved into separating gel phase, followed by 22 mA per gel for approximately one hour. Gel was transferred into gel cassette and

transfer buffer (50 mM Tris, 0.38 M glycin, 20 % methanol, 0.1 % SDS) was added. An ice unit and ice box were provided to keep temperature low during transfer. Running time was 2 hours at 300 mA. When finished, membrane (Nytran Supercharge Nylon Transfer Membrane, Sigma-Aldrich) was shortly rinsed with TNT (10 mM Tris HCl pH 8.0, 150 mM NaCl, 0.05 % Tween 20) to release methanol.

6.6. Activity Assays

Activity Assays were performed to measure PAR synthesis by PARP from lysates of different cancer cells. PARP in samples was activated with substrate and activator dsDNA to induce PAR production in order to determine enzymatic parameters.

Reactions were performed at 30 °C and 450 rpm shaker setting. A mix of reaction buffer (100 mM Tris HCl pH 8.0, 10 mM $MgCl_2$), DTT (1 mM), substrate NAD^+ (varying concentration from 0 to 200 µM) and dsDNA activator oligonucleotide (GGAATTCC, 25 µg/ ml) was prepared and pre-warmed to 30 °C for 2 minutes before adding $1/10^{th}$ volume of sample (according to Beneke et al., 2010). Reaction time varied between 30 seconds and 3 minutes in order to determine suitable PAR production. Reactions were stopped by adding an equal volume of ice cold 20 % TCA. Control samples without NAD^+ additive were treated with 20 % TCA first before adding PARP in order to avoid possible reactions. Samples and PAR Standard were diluted further in 10 % TCA for loading. Slot blots were set up with three (Minifold II, Schleicher & Schuell, Inc.) to five (Bio-Dot SF, Bio-Rad) Whatman papers and an Amersham Hybond-N+ membrane (GE Healthcare), whereas membrane and two papers were previously wet in PBS. First, 100 µl PBS were aspirated, followed by 100 µl sample, 100 µl 10 % TCA and finally 100 µl 70 % ethanol. Membrane was dried at 80 °C in an UF30 incubator (Memmert) for one hour before blocking membrane with 5 % milk in TNT.

6.7. PARP1 and PAR Detection

The following protocol was used for both Western blot and slot blot membranes. Incubation started in 5 % milk/ TNT slowly shaking either overnight at 4 °C or for 2 hours at room temperature. Subsequently membrane was incubated with first antibody (in 5 % milk/ TNT) on slow shaker mode for one hour at room temperature or overnight at 4 °C. First antibodies were 10H (1:600, isolated from mouse hybridoma cells) for PAR, C2-10 (1:2000, Santa Cruz Biotechnology) or FI23 (1:5 supernatant of mouse hybridoma cells) for PARP1 detection. The PAR recognizing antibody 10H has been shown to be monoclonal and binding PAR chains consisting of over 20 units (Kawamitsu et al., 1984). Afterwards membranes were washed in TNT three times for 15 minutes each at high shaking mode until second antibody was applied: goat anti mouse antibody (1:20,000, Sigma) for 45 minutes at room temperature on slow shaker; followed again by three washings with TNT, each 15 minutes. Membranes were developed using the Intelligent Dark Box by Fujifilm and the computer program LAS3000. For chemoluminescence reaction SuperSignal West Femto Maximum Sensitivity Substrate (Thermo Scientific) or Amersham ECL Select Western Blotting

Detection Reagent (GE Healthcare) was applied with a 30 seconds pre-incubation time.

6.8. Intensity Analysis

Slots were analyzed with ImageJ and Excel. On each membrane a PAR standard was applied in order to normalize intensity values of samples. Blank slots were used as background values. In cases of uneven membrane backgrounds, each sample received its own adjacent background measurement.
In Excel background values were subtracted from each sample intensity value, resulting solely in sample intensity. Means were calculated from technical triplicates. Finally samples were normalized first to the applied standard (PAR standard for slot blots and wild type PARP1 for Western blot PARP1 analysis) and second either to the sample's protein amount (lysis protocol comparison) or cell count (slot blots and PARP1 comparison in different cancer cells). Data was transferred to Graph Pad Prism 6 for graphs and activity parameter calculations (activity assays).

6.9. Modifications to Protocols

During the course of the dissertation, several adjustments to the initial protocols were made. The different rationales are given in the results section.

6.9.1. Protamine Sulfate versus DNase I

As alternative to eliminate DNA during lysis, Protamine sulfate was replaced by DNase I (AppliChem). Supernatants 1 were incubated with DNase I at different concentrations varying from 0.19 units up to 7.5 units per µl supernatant. Reaction mixes consisted of cell lysate, reaction buffer (50 mM Tris HCl pH 7.5, 10 mM $MgCl_2$, 50 µg/ ml BSA), $CaCl_2$ (10 mM) and respective DNase I amount. Incubation time was one hour at 37 °C and 550 rpm. Degree of DNA digestion was determined on an agarose gel and PARP1 integrity through Western blot.

6.9.2. Dialysis versus Filtration

The process of dialysis is time consuming and was to be replaced. As fast and easy alternative, samples were filtered through Amicon Ultra 0.5 ml Centrifugal Filter Devices (30 K, Millipore). Supernatants were applied and devices spun at 14,000 x g for 10 minutes at 4 °C to collect PARP1 in filters. For washings one volume of PBS was loaded onto filters and tubes were centrifuged again. Washing step was repeated once and flow-throughs were discarded. To receive filtrates, filter devices were placed upside down into new tubes and centrifuged at 1000 x g for 2 minutes at 4 °C. Concentrates were resuspended to original volume with 20 % glycerol/ PBS. Samples were frozen in liquid nitrogen and stored at -80 °C until further needed for comparative activity assays. In addition to verify the necessity of a dialysis or filtration step, final supernatants were directly used for activity assays without any further processing.

6.9.3. TCA versus PBS

To consider any effects TCA might have on PARP1 and formed PAR, a protocol adjustment was made. Standard assay protocol uses 20 % TCA to stop PAR forming reactions and 10 % TCA to dilute samples for slot blotting. Alternatively to TCA denaturation of PARP proteins, PJ-34 was used to stop the reactions: an equal volume of ice cold PJ-34 (20 µM in PBS) was added to samples after reaction time elapsed, immediately followed by freezing samples in liquid nitrogen. The freezing process without any glycerol to stabilize and protect proteins in the sample is thought to prevent further PAR formation or degradation after end of reaction. For slot blotting samples and PAR standard were diluted in PBS.

6.9.4. Protocol Shortening

For PAR forming activity of intact cells, cells were treated with PJ-34 and/ or H_2O_2, lysed and slot blotted. LPSC lysis originally consisted of an incubation time of 20 minutes followed by two centrifugation steps. However, it is possible that formed PAR is degraded in the long process of lysis. For this reason two shortened protocols were tested. Cell pellets contained the same amount of cells ($1 \cdot 10^6$ cells) and were resuspended in a fixed volume of PBS. PJ-34 (5 µM) and/ or H_2O_2 (2 mM) was added to cell suspension and incubated at normal conditions (5 minutes at 37 °C and 450 rpm). Reactions were stopped by freezing samples in liquid nitrogen. Controls were left untreated and frozen directly. For lysis one volume of 2x LPSC buffer mix was added. One protocol continued with the incubation and first centrifugation while second protocol skipped these steps. All samples were then diluted in PBS and lysed cell suspensions were loaded onto slot blot.

6.10. PARP Inhibitor and H_2O_2 Treatment of Cells

After establishing the most suitable lysis protocol and determining PARP activity parameters in different cancer cells, PAR formation in the cell itself upon challenge with H_2O_2 as well as necessary PJ-34 concentration to fully block PARP activity were investigated. H_2O_2 and PJ-34 treatments were carried out with the following cancer cells: HeLa, U2OS, SH-SY5Y, MCF-7 and HepG2. Since PAR is quickly degraded the shortened LPSC protocol as mentioned above (no incubation or centrifugation) was applied. Treatments were conducted with cell pellets of each $1 \cdot 10^6$ cells. Resuspended in PBS, H_2O_2 or combined PJ-34/ H_2O_2 treatments were performed at 37° C and 450 rpm for 5 minutes. For H_2O_2 and PJ-34 concentrations see Table 5. Reactions were stopped by freezing samples in liquid nitrogen.

Sample	1	2	3	4	5	6	7	8	9	10
H_2O_2	5 mM	3 mM	2 mM	1.5 mM	1 mM	0.5 mM	0.2 mM	0.1 mM	0	control
PJ-34	2 µM	1 µM	0.8 µM	0.7 µM	0.6 µM	0.4 µM	0.2 µM	0.1 µM	0	-
H_2O_2	0.2 mM	0.2 mM	0.2 mM	0.2 mM	0.2 mM	0.2 mM	0.2 mM	0.2 mM	0.2 mM	-
PJ-34	2 µM	1 µM	0.8 µM	0.7 µM	0.6 µM	0.4 µM	0.2 µM	0.1 µM	0	-
H_2O_2	2 mM	2 mM	2 mM	2 mM	2 mM	2 mM	2 mM	2 mM	2 mM	-

Table 5: Treatment conditions and concentrations. For H_2O_2 or PJ-34 free samples (9 and 10) PBS was added instead in same volumes. Control samples did not react and were frozen in liquid nitrogen immediately to account for basal PAR levels in cells.

6.11. Viability Assays

To analyze differences in cell viability towards the cytotoxic substances H_2O_2 and temozolomide (Sigma-Aldrich), resazurin-based (Alfa Aesar) Alamar Blue Assays were conducted with HeLa, U2OS, SH-SY5Y, MCF-7 and HepG2 cancer cells. In addition the effect of PJ-34 combined with these DNA damaging agents was tested. 96 well plates with $1 \cdot 10^4$ cells/ well were used in the assays. H_2O_2 and temozolomide concentrations were diluted in respective cell media and applied in triplicates (technical and biological). Dilution series and plate compositions are seen in Figure 1. Periods for H_2O_2/ temozolomide incubation and reduction were 24 and 3 hours, respectively. Reduction intensities were measured with LS55 Luminescence Spectrometer (Perkin Elmer) and FL Winlab (Uptiblue Program with an excitation of 560 and emission of 590 nm). Results were analyzed with Excel and Graph Pad Prism 6. Of every intensity the respective background (with or without PJ-34) was subtracted. Furthermore, for temozolomide trials each value was divided by a control sample containing DMSO, as temozolomide powder was solved in DMSO.

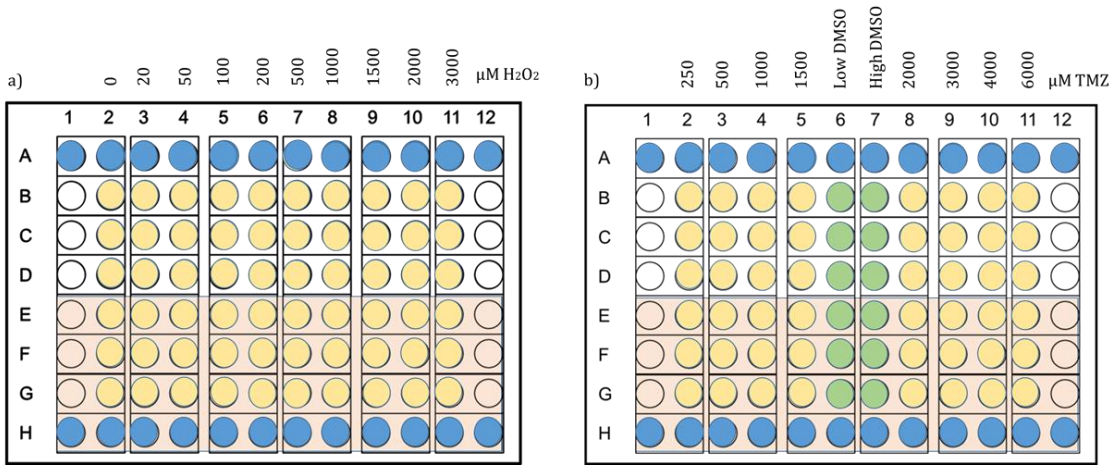

Fig. 1: 96 well plate composition and dilution series for Alamar Blue Assays. Lower halves (red) were pre-incubated with PJ-34 (5 µM) for 5 minutes before adding cytotoxic agents. Blue wells indicate background wells: row A for upper and row H for lower half of plates. Yellow wells were treated with different concentrations of H_2O_2 (a) or temozolomide (TMZ, b). Control wells (b, green) were incubated with DMSO; low DMSO corresponds to DMSO concentration in 250 µM temozolomide and high DMSO to 6000 µM temozolomide treated samples.

7. RESULTS

7.1. Comparison of Lysis Protocols

LPSC, CHAPS, RIPA, modified CHAPS and modified RIPA lysis protocols were compared regarding PARP1 yield with complete extraction of PARP1 from chromatin and preservation of enzymatic activity. Reaction steps are depicted in Figure 2. Original CHAPS and RIPA protocols ended with supernatant 1, whereas LPSC, modified CHAPS and modified RIPA protocols continued to supernatant 2.

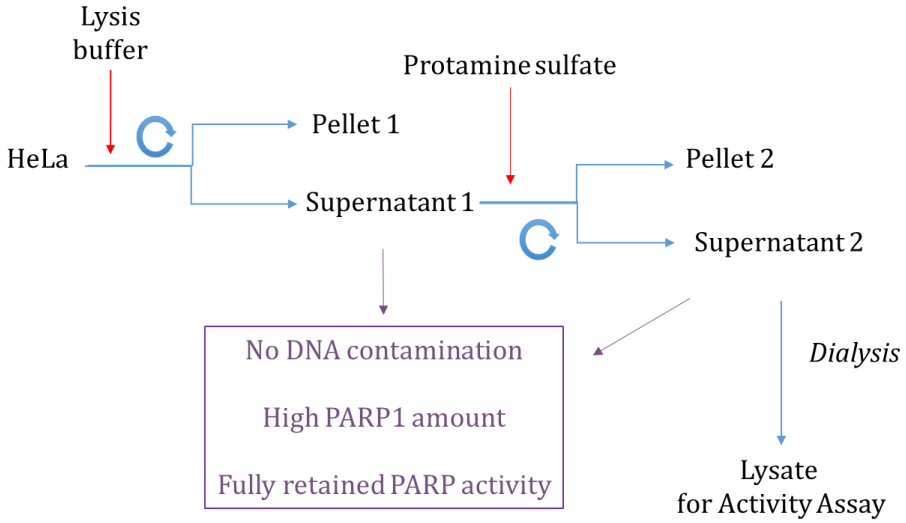

Fig. 2: Overview of reaction steps of cell lyses. Purple features indicate the ideal final supernatant.

7.1.1. PARP1 Loss:

To compare PARP1 loss, samples were taken at every step of the lysis protocols for Western blots. Supernatants and pellets (re-solubilized in PBS) were loaded to check for PARP1 loss into the pellets.

Original CHAPS protocol showed PARP1 in pellets even with addition of urea (Fig. 3a). However, modified versions of CHAPS and RIPA as well as LPSC did not display PARP1 signals in pellet fractions (Fig. 3b).

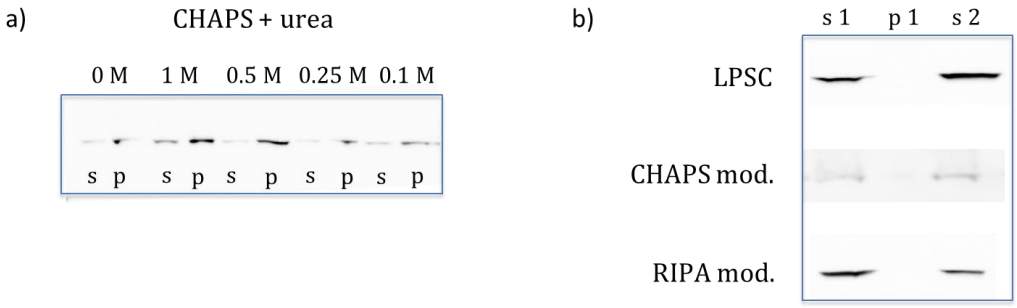

Fig. 3: PARP1 loss into pellets. a) CHAPS protocol with urea concentrations from 0 to 1 M. b) LPSC and modified protocols. s = supernatant, p = pellet

7.1.2. PARP1 Yield Relative to Protein Amount

Protein measurements and Western blots were performed with supernatants 2 after dialysis. Identical numbers of HeLa cells as starting material yielded higher PARP1 protein amount with LPSC compared to modified CHAPS and modified RIPA protocols (Fig. 4). However, relative to total protein, modified CHAPS contained the highest relative PARP1 concentration (Table 6).

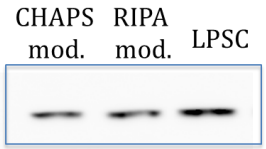

Fig. 4: PARP1 level in supernatants 2.

	Total Protein [µg/ µl]	PARP1 Amount [ng/ µl]	Rel. PARP1 Amount [%]
LPSC	0.27	1.96	0.73
CHAPS mod.	0.09	1.23	1.41
RIPA mod.	0.2	1.07	0.54

Table 6: PARP1 level in relation to total protein amount. Total protein and PARP1 amount are per µl lysis buffer.

7.1.3. Remaining Genomic DNA

To perform activity assays as controlled as possible, samples should be devoid of any contaminating genomic DNA. Residual DNA can activate PARP1 and influence activity assay results. An agarose gel was performed and showed only LPSC and modified CHAPS to be free of genomic DNA (Fig. 5). In final supernatants of other protocols remnants of DNA were found.

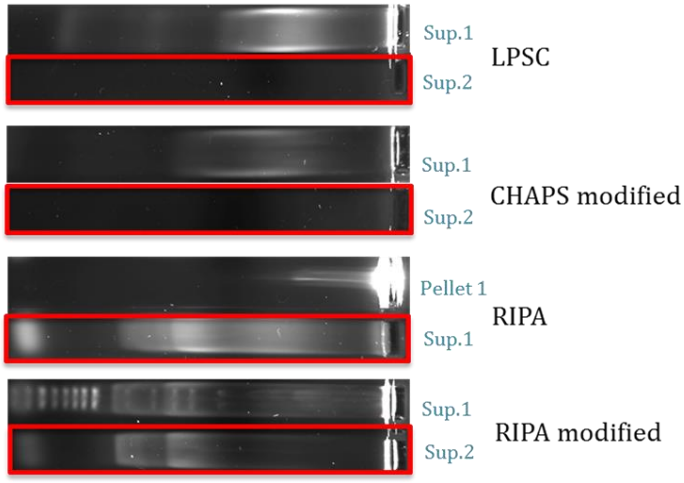

Fig. 5: Remaining DNA amounts in final supernatants. Loaded sample volumes of supernatants correspond to similar cell counts for all except LPSC (approx. $3.7 \cdot 10^4$ cells versus $9.4 \cdot 10^4$ cells, respectively). s = supernatant, p = pellet

7.1.4. PARP Activity

Activity assays were performed with dialyzed supernatants 2. Apparently LPSC samples displayed the strongest signal on membrane (Fig. 6a). After normalizing to the same amount of PARP1 to account for unequal PARP1 extraction (see PARP1 yield above), LPSC lysed cells had highest PARP activity followed by modified CHAPS (Fig. 6b). PARP from RIPA lysed cells was least active.

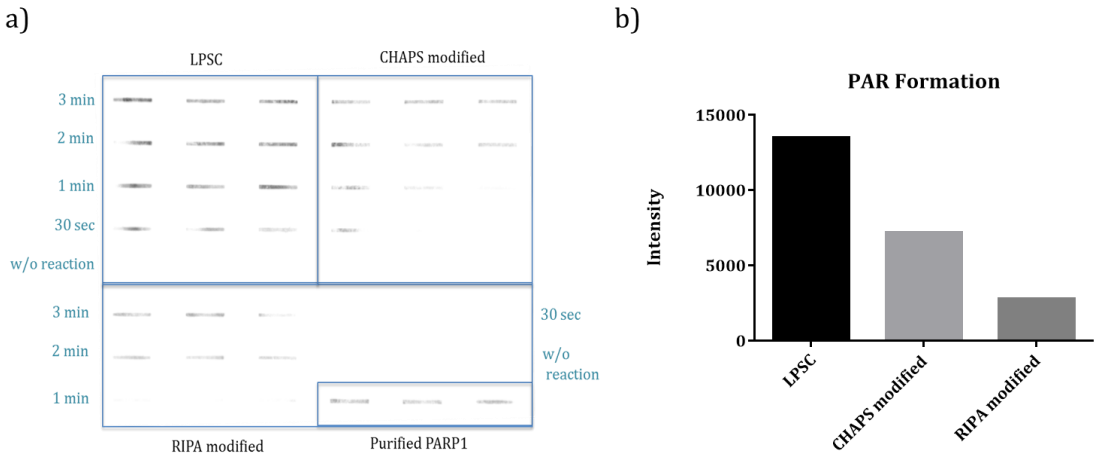

Fig. 6: a) PAR formation at 200 µM NAD^+ from cells lysed with different protocols. Reaction with purified recombinant PARP1 was used as positive control b) Comparison of activities at 1 minute reaction time, intensities normalized to the same PARP1 amount.

7.2. Modifications of LPSC Protocol

7.2.1. Reaction Time

Several activity assays were performed to determine the final experimental conditions. In order to define a suitable reaction time NAD^+ concentration series (0, 10, 20, 50, 100, 200, 400 µM) were combined with different reaction times of 30 seconds, 1, 2 and 3 minutes. Figure 7 shows the results for varying reaction times. All slopes start off steep before reaching a plateau-phase. Magnification of the lower axis area (Fig. 7 blue box) underlines the sigmoidal shape of all graphs at low NAD^+ concentrations, typical for the second order kinetics of PARP1.

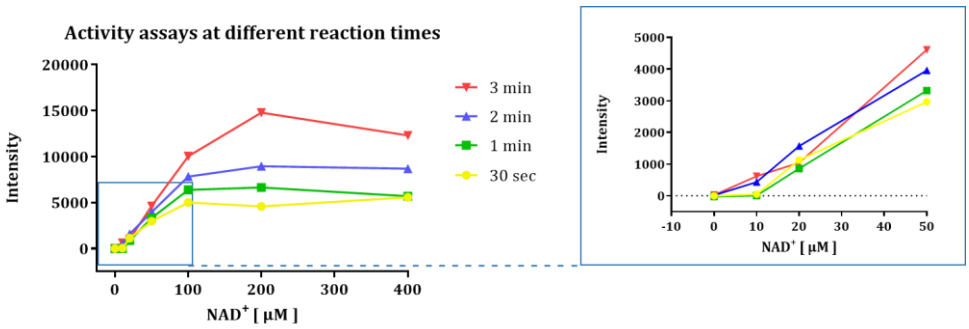

Fig. 7: PARP activity assays with varying reaction times. Blue box magnifies axis area at lower NAD^+ concentrations.

7.2.2. PAR Stability During Lysis

To investigate impacts of lysis protocol on PARP1 integrity and baseline PAR, HeLa cells were treated with PJ-34 and H_2O_2 alone or in combination before LPSC lysis.

Old medium from culture plates was discarded and cells were washed with PBS. One group was treated with the PARP1 inhibitor PJ-34 (20 mM end concentration in medium; Enzo Life Sciences) for 10 minutes, the others with medium only. After PJ-34 was removed, a 10 minute H_2O_2 (1 mM in medium; 30% stock by Roth) treatment followed. Finally medium was replaced by trypsin and after 5 minutes at 37 °C cells were harvested. A second group was treated with PJ-34 only, while yet another with H_2O_2 only. An untreated sample served as control. To include cells in lysis that possibly died through H_2O_2 treatment, old medium was used to harvest respective samples after trypsin incubation. Cells were counted and pelleted by centrifuging at 2,500 x g for 5 minutes at room temperature. Supernatants were discarded and cell pellets washed with PBS before centrifugation as above. Cells were finally lysed by LPSC. Input, supernatant 1 and supernatant 2 were loaded for Western blots.

PAR formation is visible for untreated and H_2O_2 treated cells only (Fig. 8). Unexpectedly PAR levels in supernatant 1 are different from supernatant 2: nucleic acid precipitation by Protamine sulfate led to a major PAR loss in both samples.

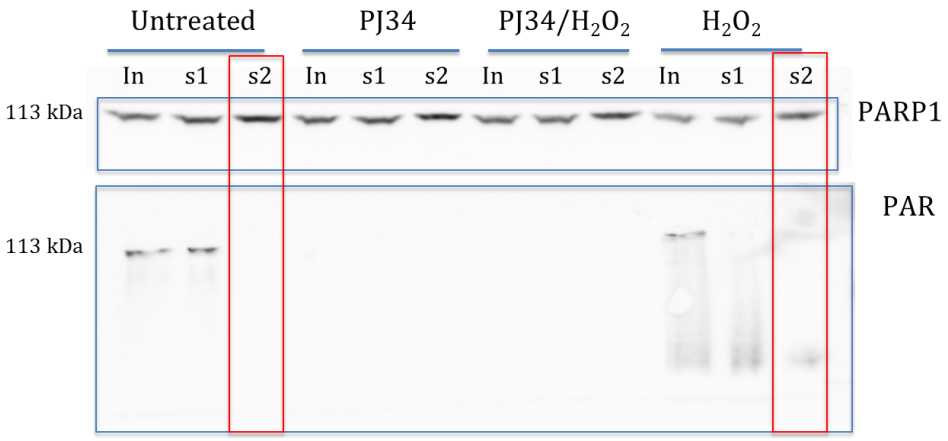

Fig. 8: PARP1 and PAR stability during each lysis step. PAR detection for untreated and H_2O_2 treated samples only. Whereas PARP1 amount is not influenced, there is a decline of PAR slightly in supernatant 1 and obviously in supernatant 2 (red boxes). In= input, s1/2= supernatant 1/2

7.2.3. Protamine Sulfate versus DNase I

The data in Fig. 8 suggest that DNA elimination by Protamine sulfate during lysis also induces precipitation of PARylated proteins, probably due to the nucleic acids-like nature of PAR. Thus, this step was replaced by DNase I treatment to avoid PAR loss and tested for efficiency of DNA degradation. Supernatants 1 were incubated with different concentrations of DNase I varying from 0.19 units to 7.5 units per µl supernatant. After an incubation of 1 hour at 37 °C and 550 rpm, the degree of DNA digestion and PARP1 integrity were tested on an agarose gel and by Western blotting, respectively.

DNA digestion was dose-dependent, but only down to fragment sizes of 10 -1000 bp even at the highest DNase I concentration (Fig. 9a, samples 5 and 6). However, DNase I levels of more than 0.19 units/ µl supernatant lead to PARP1 cleavage (Fig. 9b, samples 2-6), probably due to DNase I contamination with proteases. Therefore, DNase treatment did not have the anticipated result and was dismissed in further experiments.

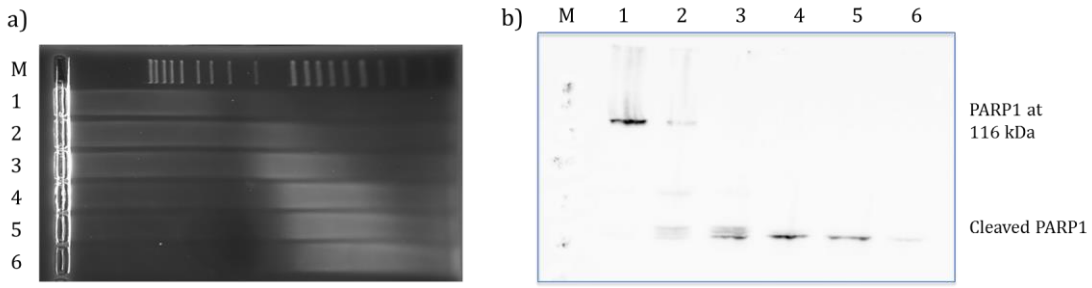

Fig. 9: a) DNA digestion by DNase I: DNA was degraded dose-dependently, but even at high DNase I concentrations only to fragments between 10 and 1000 bp. b) PARP1 integrity after DNase I incubations: PARP1 cleavage is induced at 0.375 units and above. M = Marker, 1-6 increasing amounts of DNase I (0.19, 0.375, 0.75, 2.25, 3.75 and 7.5 units/ µl supernatant).

7.2.4. Dialysis versus Filtration

To compare the influence of dialysis and filtration on PARP activity, activity assays were performed with LPSC lysed cell samples that were filtered through a spin column, dialyzed against 20% glycerol/ PBS, or used directly.

Under equal conditions dialyzed samples had a higher PAR capacity compared to filtered (Fig. 10a) and untreated (Fig. 10b) ones. This suggests PARP1 protein loss by filtration or inhibition by components of the isolation buffer. As dialysis is a time consuming step in the original isolation protocol (overnight), and as unprocessed samples still yielded measureable signals in activity assays, the dialysis was excluded from the further protocol strategy.

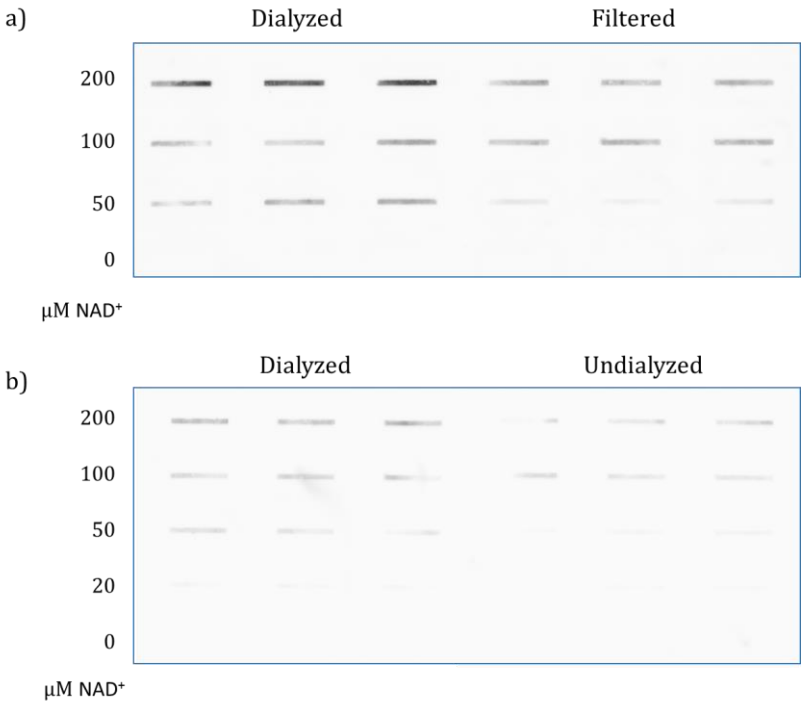

Fig. 10: PAR forming reactions in triplicates at various NAD^+ concentrations with differently processed samples: a) dialyzed versus filtered b) dialyzed versus untreated.

7.2.5. TCA versus PBS

PAR synthesis in activity assays was satisfying. However, basic cellular PAR was hardly detectable in control samples (0 µM NAD^+). Figure 11 displays the effect of a protocol change, by replacing TCA precipitation with addition of one volume PJ-34 (20 µM) in PBS to stop the reaction: PJ-34/ PBS samples show stronger PAR signals (Fig. 11a). Additionally, at higher developmental times preformed PAR was detectable in PJ-34/ PBS control sample (Fig. 11b red box).

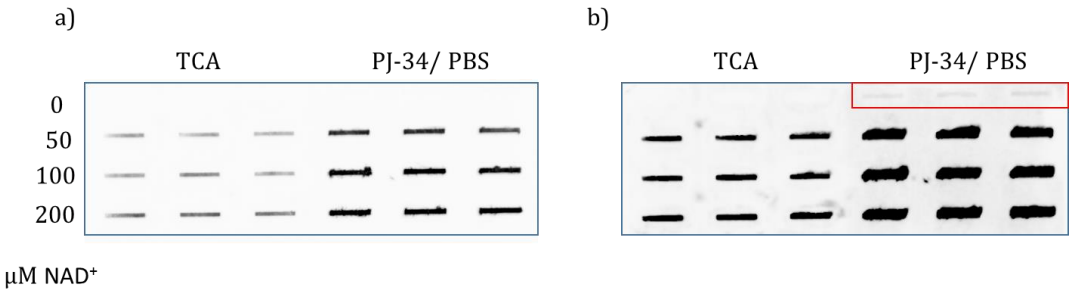

Fig. 11: Activity assay results performed with standard procedure (TCA) versus adapted protocol (PJ-34/ PBS) with PJ-34 to stop reactions and PBS for sample dilution prior to loading. b) Same membrane after longer development presents preformed PAR for PJ-34/ PBS sample (red box).

7.3. Activity Assays

Enzyme parameters (K_M and V_{max}) for PAR synthesis from different cancer cell lines were determined with activity assays. Cell lysates were generated by LPSC lysis including the protocol changes described above: samples were lysed by incubation in LPSC buffer for 20 minutes at 4 °C. After first centrifugation at 4 °C two volumes of 30 % glycerol/ PBS were added to supernatants to stabilize proteins for subsequent freezing in liquid nitrogen. Samples were stored at -80 °C until needed for assays. In reactions cell lysates ($1/10^{th}$ total volume) were incubated with increasing NAD^+ concentrations and reaction time was set to one minute. Instead of using TCA as described in the original protocol, reactions were stopped with one volume ice cold PJ-34 (20 µM in PBS) and samples were diluted in PBS prior to loading. An overview of the final protocol version is given in Figure 12. For each cell line a minimum of five assays were performed. Blotting, drying and blocking procedures remained unchanged.

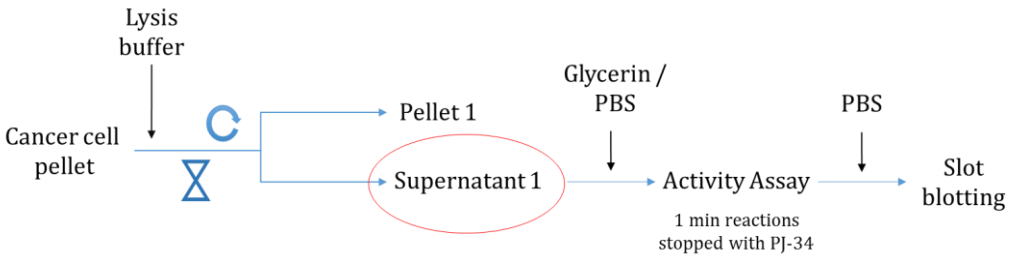

Fig. 12: Overview of reaction steps for activity assays. ⧖ Incubation, ↻ Centrifugation

Results for each cell line are displayed in Figure 13. HeLa, MCF-7 and SH-SY5Y graphs demonstrate a sigmoidal shape at lower NAD^+ concentrations. After a short phase of linear increase in PAR, graphs flatten at higher concentrations until they reach a plateau-phase of maximal PAR concentration. While HeLa and MCF-7 cells have a final PAR production of around 1050 pmol / 10^6 cells, U2OS and SH-SY5Y cells produced 716 and 642 pmol / 10^6 cells, respectively, followed by HepG2 with only about half the amount as the first two cell lines. However, HepG2 already displayed detectable background levels of PAR in cells. Lowest constitutive PAR level was measured for HeLa cells (1.7 pmol / 10^6 cells), followed by SH-SY5Y, U2OS, HepG2 and finally MCF-7 cells (48 pmol / 10^6 cells).

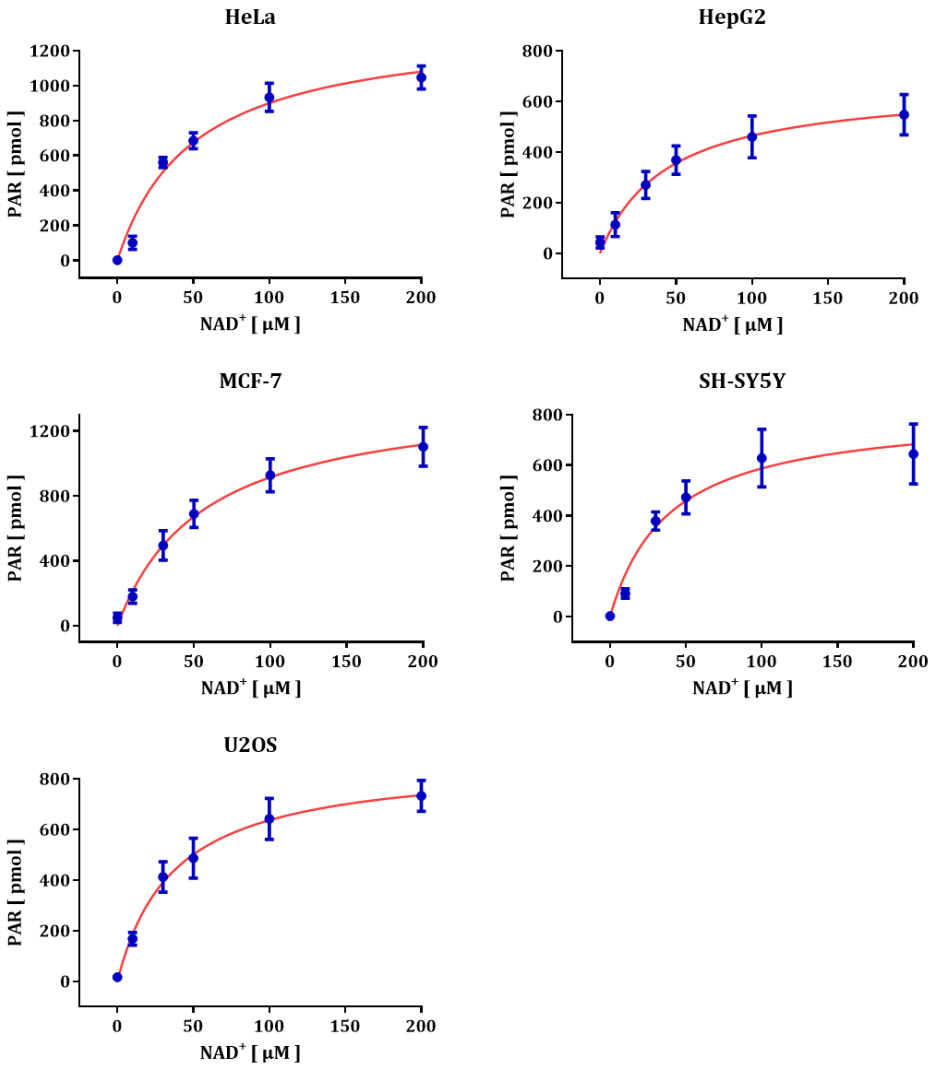

Fig. 13: Means with SEM of activity assays for different cancer cell lines (blue). Michaelis-Menten kinetics calculated for each graph (red).

Enzyme kinetics and statistical significance are summarized in Table 7. A t-test revealed significant differences in V_{max} for HeLa/ HepG2, HeLa/ SH-SY5Y, HeLa/ U2OS, HepG2/ MCF-7 and MCF-7/ SH-SY5Y cell lines. K_M values did not differ significantly.

V_{max} & K_M	HeLa	HepG2	MCF-7	SH-SY5Y	U2OS
HeLa	1361.2 & 51.2	0.8605	0.3977	0.1703	0.945
HepG2	0.001	678.1 & 49.5	0.3783	0.2385	0.8782
MCF-7	0.4122	0.0127	1622.5 & 85.1	0.1678	0.4511
SH-SY5Y	0.0407	0.4752	0.0303	838.5 & 37.4	0.3748
U2OS	0.0184	0.0706	0.0520	0.644	942.7 & 52.4

Table 7: Overview of V_{max} and K_M as well as respective p-values of the different cancer cell lines. Diagonal white boxes display V_{max} and K_M values. Values with dark gray background represent p-values for V_{max} and those with light gray background p-values for K_M. Red numbers indicate p-values of statistical significance.

7.4. PARP1 Amount in Cancer Cell Lines

For comparison of PARP1 levels in different cancer cells, $1 \cdot 10^6$ cells were lysed according to lysates for activity assays (see above). However, no glycerol/ PBS was added and instead lysates were directly loaded for Western blotting (for protocol and loading dye composition see 6.5. Western Blotting). PARP1 amounts for cell lines were calculated by comparison with a sample of recombinant PARP1.

Figure 14 shows different PARP1 protein expression in tested cancer cell lines. There is distinct variation in PARP1 amount, ranging from 28.4 ng / 10^6 cells for U2OS to 178 ng / 10^6 cells for HeLa. A t-test revealed significant differences for HeLa/ HepG2 ($p = 0.0087$), HeLa/ MCF-7 ($p = 0.0106$), HeLa/ SH-SY5Y ($p = 0.0001$), HeLa/ U2OS ($p = 0.0001$), HepG2/ U2OS ($p = 0.0115$), MCF-7/ SH-SY5Y ($p = 0.0067$), MCF-7/ U2OS ($p = 0.0008$) as well as for SH-SY5Y/ U2OS ($p = 0.0375$).

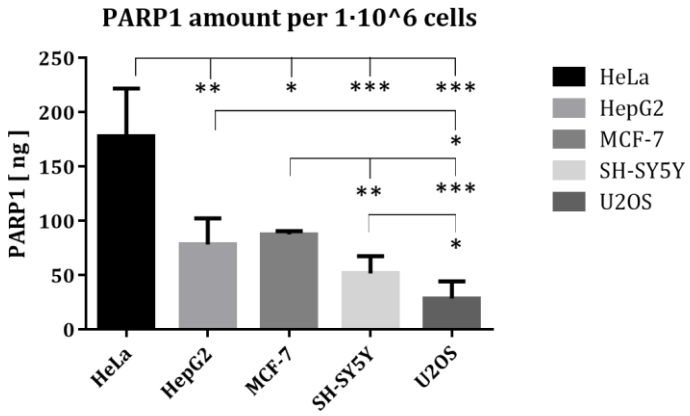

Fig. 14: PARP1 amounts per $1 \cdot 10^6$ cells compared to recombinant PARP1. Means and standard deviation are displayed. Stars represent levels of significance between two cell lines connected by line.

7.5. Protocol Shortening

In terms of in-cell treatments with PAR formation, LPSC lysis protocol still needed to be optimized since a previous experiment (7.2.2. Fig. 8) indicated PAR loss already during first lysis steps. Thus, to ensure extraction of background cellular PAR, lysis protocol was improved further.

After resuspending cell pellets in one volume of PBS, cells were treated with PJ-34, H_2O_2 and in combination. The reaction was stopped by snap-freezing the samples in liquid nitrogen. Subsequently, one volume of 2x LPSC buffer mix was added. To test for alterations in PAR yield, one protocol went on with 20 minutes incubation followed by centrifugation, whereas the other left out any further lysis steps. Finally, samples were diluted in PBS and loaded onto slot blot.

Figure 15 displays membranes of the two protocol modifications. PAR is undetectable in cells treated with PJ-34 or with PJ-34 in combination with H_2O_2. Unexpectedly, there is distinct PAR formation in the control and only slight PAR for the H_2O_2 treated sample in the elaborated protocol (Fig. 15a). The shorter protocol displays the expected strong PAR signal in H_2O_2 treated samples, which is abrogated by PJ-34 pre-incubation. Of note, control samples display low-levels of preformed PAR (Fig. 15b).

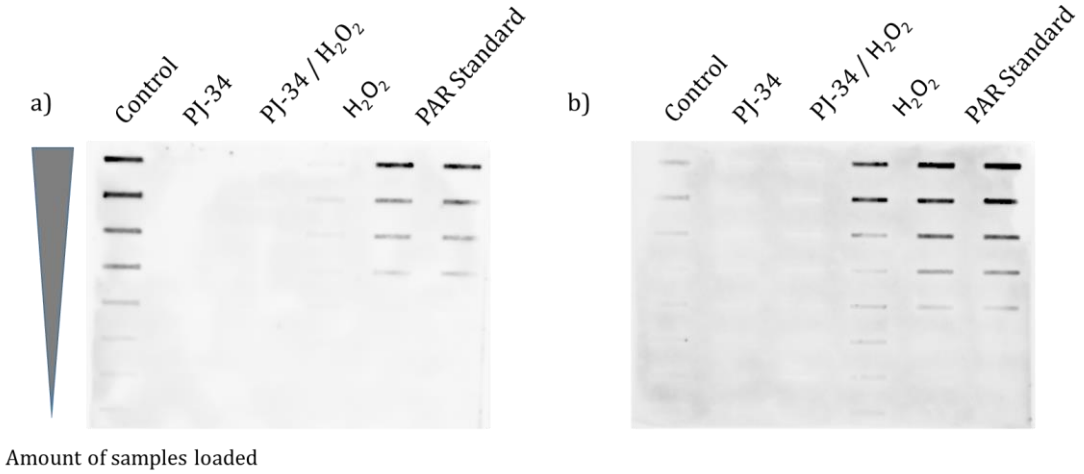

Fig. 15: Visible PAR formation of differently treated cells after lysing protocol with incubation and centrifugation (a) and protocol without (b).

7.6. H_2O_2 Treatment of Cells

With this modification to the standard lysis protocol for activity assays, in-cell PAR formation could be detected in sufficient intensity. Cells were treated with H_2O_2 and snap-frozen to stop the reactions, before adding LPSC lysis buffer. Incubation and centrifugation were left out to avoid PAR degradation. Diluted in PBS, lysates were directly loaded onto slot blots.
Cell treatment results are seen in Figure 16.

a)

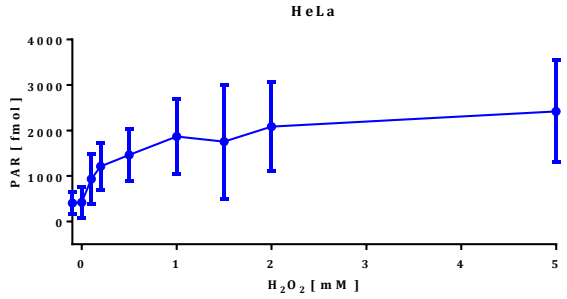

b)

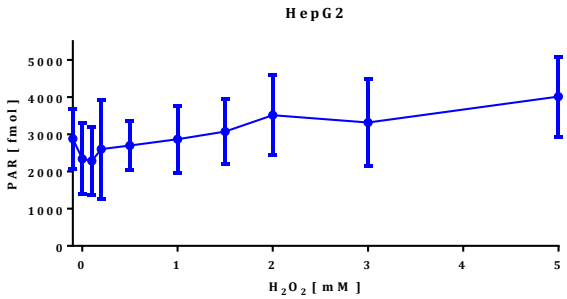

c)

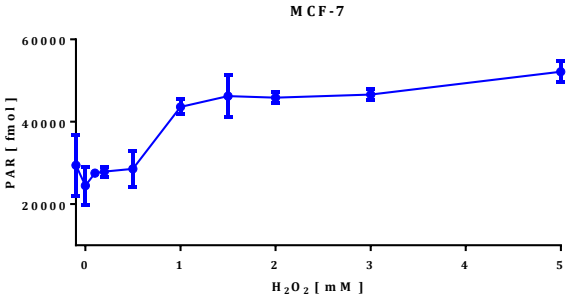

d)

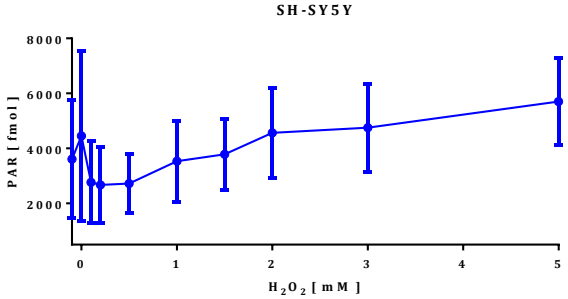

e)

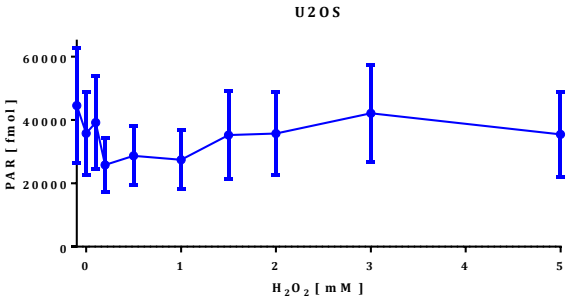

Fig. 16: Means with SEM of PAR production for H_2O_2 treatments. For each cancer cell line $1 \cdot 10^6$ cells were used per treatment. Basic PAR levels are displayed on y-axis. **a)** Starting with a low constitutive PAR level around 404 fmol, HeLa cells reach a maximum PAR production of around 2.4 pmol when challenged with H_2O_2. This is almost a sixfold increase in PAR synthesis. **b)** HepG2 cancer cells show the lowest PAR forming capacity: from a basic PAR level of around 2.9 pmol to a final yield of 4 pmol PAR. **c)** H_2O_2 treatment induces highest PAR levels in MCF-7 compared to other cell lines. As base-line PAR is also very high, relative induction is only almost twofold. **d)** For SH-SY5Y cells PAR amount at highest H_2O_2 challenge and basic PAR level differ by factor 1.6. **e)** U2OS cells demonstrate the highest basic PAR of the cell lines. However, PAR formation upon H_2O_2 challenge is very inconsistent and may need some refinement in assay procedure.

Interestingly, all cell lines displayed a wide variation in constitutive PAR levels. In H_2O_2 treatments highest PAR amount was produced by MCF-7 cells (22.7 pmol) and lowest by HepG2 (1.1 pmol). HeLa cells demonstrated greatest PAR forming capacity (factor 6 from basic PAR level), whereas increase in U2OS was only 1.2 fold.

7.7. PARP Inhibitor and H_2O_2 Treatment of Cells

Cells were treated with a combination of PARP inhibitor and H_2O_2. Subsequently samples were treated according to H_2O_2 treatments (see 7.6.) with snap-freezing and lysing. Again, incubation and centrifugation steps were left out to prevent the degradation of PAR.
Figure 17 shows the results of the cell treatments.

a)

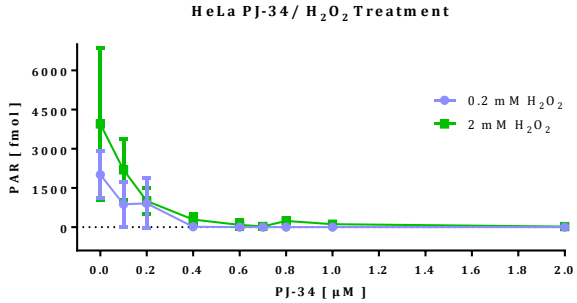

b)

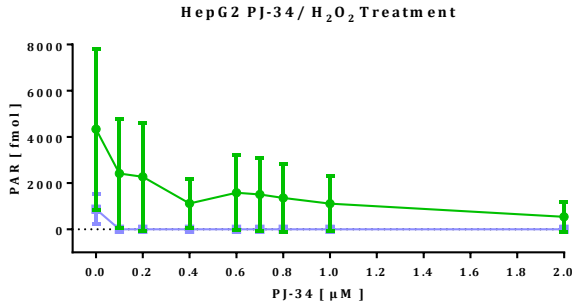

c)

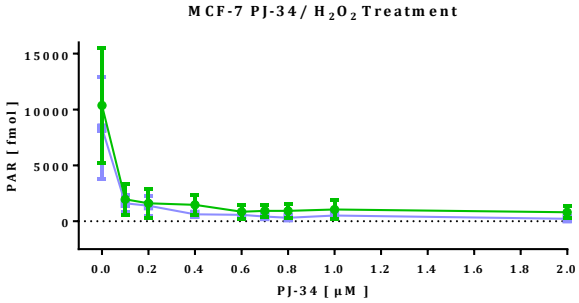

d)

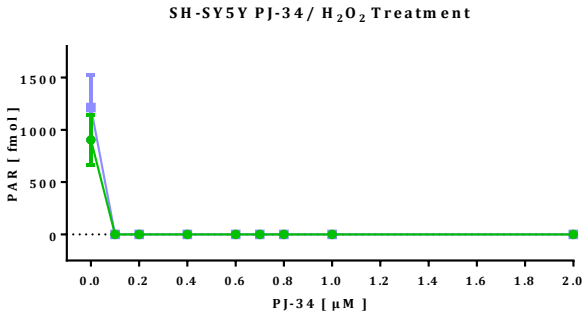

e)

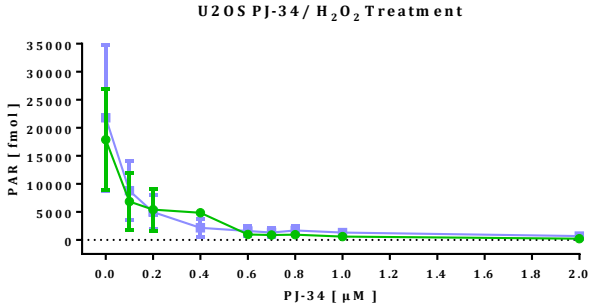

Fig. 17: Using the conditions and data obtained in Fig. 16, inhibitor application experiments were performed, using a concentration range of PJ-34 in combination of two different doses of H_2O_2. Green graphs represent 2 mM and blue graphs 0.2 mM H_2O_2 concentrations. **a)** PAR formation in HeLa cells is fully blocked at PJ-34 concentrations higher than 1 µM independent of the applied H_2O_2 concentration. **b)** While at 0.2 mM H_2O_2 the lowest inhibitor concentration is effective, the highest PJ-34 concentration is not sufficient to block PARylation completely at 2 mM H_2O_2. **c)** PJ-34 is unable to suppress PAR synthesis completely for both H_2O_2 concentrations. **d)** Already the lowest PJ-34 concentration abrogates PAR synthesis completely in SH-SY5Y cells, irrespective of H_2O_2 treatment. **e)** In U2OS cells PAR formation upon H_2O_2 challenge is only partially blocked at highest PJ-34 concentration.

Results also varied for plasticity of PARylation upon PJ-34 application. In HepG2 cells the PJ-34 amount to fully inhibit PARP differed distinctly between low and high H_2O_2 challenge. However, this was not the case for the other cell lines. While PJ-34 fully blocked PARP activity in SH-SY5Y and HeLa, PAR production was still not suppressed by highest PJ-34 concentration for U2OS and MCF-7 cells, irrespective of H_2O_2 concentration. This is most evident if the reduction by different PJ-34 concentrations is calculated in percent of the control as seen in Figure 18.

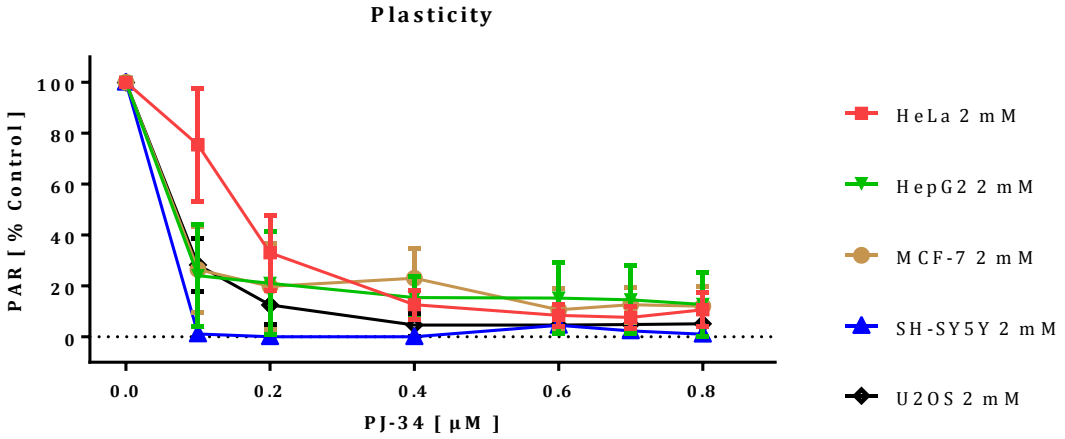

Fig. 18: Relative decrease of PAR formation at 2 mM H_2O_2 and PJ-34 combined treatment for each cancer cell line.

There is distinct reduction of PAR formation visible for most samples after PJ-34 addition. However, with increasing inhibitor dosages the degree of variation between cell lines broadens, as further decrease of PAR production distinctly varies in necessary PJ-34 amounts for cancer cells. PARP activity in SH-SY5Y cells is down to zero at 0.1 µM PJ-34, while all other cell lines level off their PAR productions slightly above zero at higher concentrations.
Variations in sensitivity of different cell lines to cytotoxic agents were investigated in viability assays with H_2O_2 and temozolomide.

7.8. Viability Assays

Response of several cancer cell lines to two different cytotoxic agents was tested with a resazurin-based viability assay. HeLa, U2OS, SH-SY5Y, MCF-7 and HepG2 cancer cells were challenged with H_2O_2 or temozolomide alone and in combination with PJ-34 (5 µM end concentration in medium). Results are displayed in Figure 19.

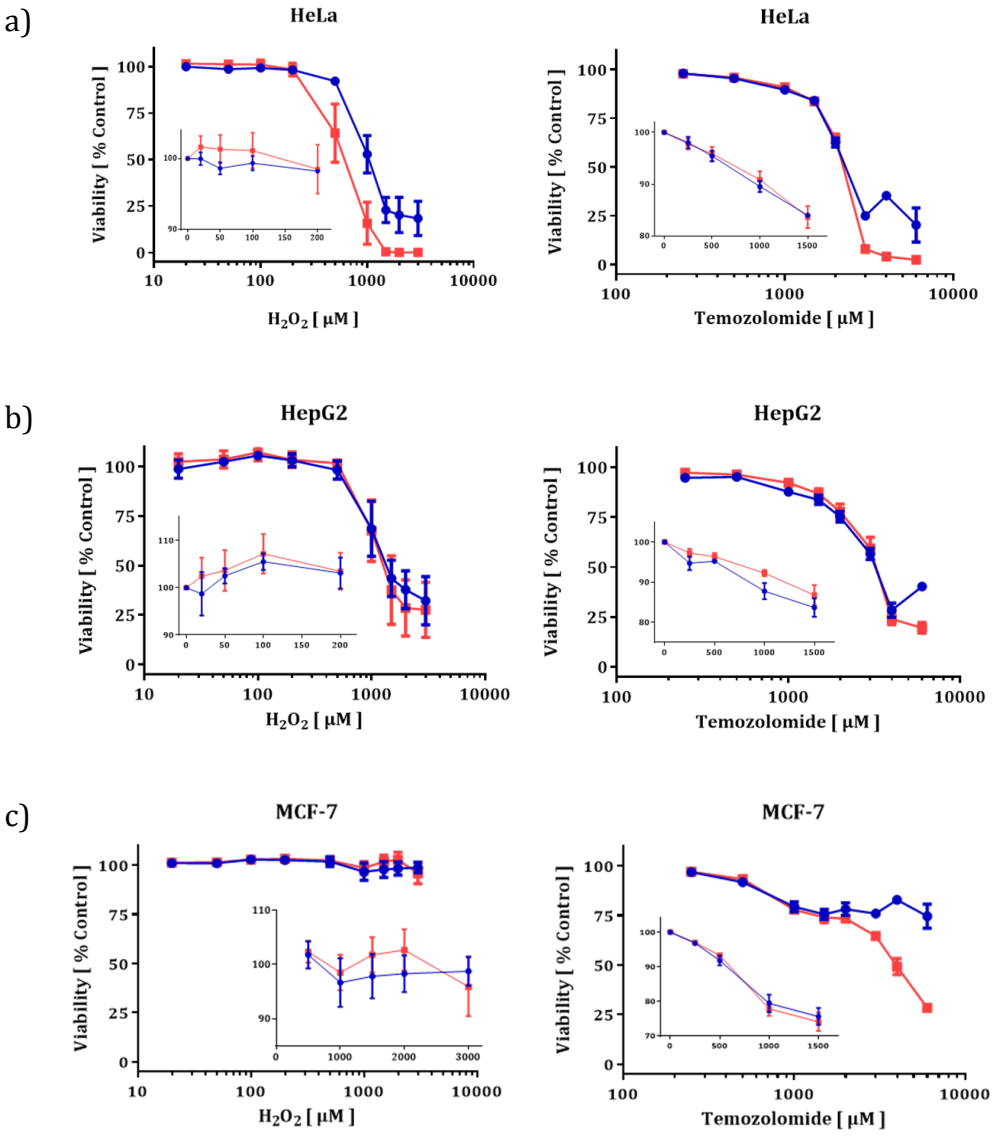

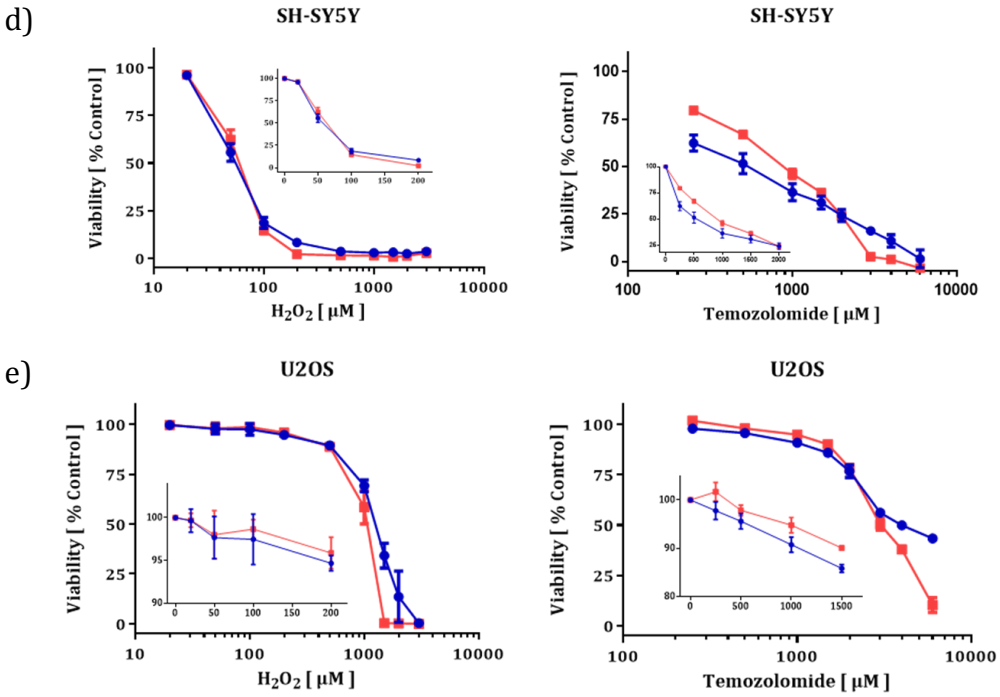

Fig. 19: Viability assays of different cancer cell lines challenged with H_2O_2 (graphs on left side) and temozolomide (right side). Both assays were combined with PJ-34 (5 µM). Blue curves indicate PJ-34/ H_2O_2 or PJ-34/ temozolomide combined treatments and red curves illustrate effect of cytotoxic agents alone. Inserted smaller graphs are magnifications of graph areas on linear scale. **a)** Higher concentrations of both cytotoxic agents lead to distinct reduction in viability in HeLa cells down to 0.1 % (H_2O_2) and 2.5 % (temozolomide). However, in combination with PJ-34 viability is sustained at about 20 %. For H_2O_2 the protective effect is established early, whereas for temozolomide it is seen only at high concentrations. The inset displays cell viability at low doses of toxins. Here PJ-34 seems to reduce viability at least in response to H_2O_2 challenge. **b)** Even without PJ-34 28 % (H_2O_2) and 20 % (temozolomide) of HepG2 cells remained viable. With PJ-34 this was slightly enhanced to 32 % for H_2O_2 and doubled for the alkylating drug. Protective effects of PARP inhibition are detected only at very high dosages; at low toxin concentrations, PJ-34 reduces viability compared to toxins alone. **c)** MCF-7 cells seem to be resistant to H_2O_2 treatment. Similar to other cell lines PJ-34 sensitizes MCF-7 to H_2O_2 treatment but not towards temozolomide. Moreover, the effect is only detectable at very high concentrations, due to inert reactions to lower H_2O_2 dosages. Compared to H_2O_2, temozolomide induces significant loss of viability in MCF-7. Application of PJ-34 has a protective effect on viability at higher doses, increasing viability threefold from 28 % (temozolomide alone) to 75 %. **d)** SH-SY5Y cells are most sensitive to cytotoxic treatment. Already 200 µM H_2O_2 is reducing viability down to zero. With temozolomide, a biphasic response with PARP inhibition can be detected. Whereas PJ-34 negatively reduces viability at low doses of the alkylating agent, it protects from temozolomide at high concentrations. **e)** At high H_2O_2 and temozolomide concentrations PJ-34 mildly protects U2OS cells from cell death. However, PARP1 inhibition decreases viability at lower cytotoxin concentrations.

In cytotoxicity treatments, results vary already within the cell lines, best seen in SH-SY5Y and MCF-7 cells, where H_2O_2 and temozolomide cause differential viability impairments. H_2O_2 treatment in MCF-7 cells seems to have almost no

effect on the cells, unlike temozolomide, which reduces viability already at 1 mM. SH-SY5Y cells display contrasting results with higher sensitivity towards H_2O_2. HeLa, HepG2 and U2OS cells demonstrated comparable sensitivities to the cytotoxic agents.

The cell lines reacted differently to PARP inhibition. While PJ-34 has no considerable effect in H_2O_2 treated SH-SY5Y cells, it displays a biphasic effect with temozolomide treatment, favoring cell death at lower but acting protective at higher temozolomide doses. In HeLa cells and H_2O_2, PJ-34 protects cells from cell death at higher toxin concentrations and to a certain degree sensitizes them at low concentrations. With temozolomide the protective effect of PJ-34 in HeLa is only apparent at very high temozolomide doses without any sensitization. In HepG2 cells the sensitization response to PJ-34 is detected with temozolomide, but not with H_2O_2, opposite to HeLa cells. Additionally, PJ-34 does not protect HepG2 at high doses of both genotoxins. U2OS cells show a similar response to PARP inhibition at low toxin doses as HepG2 cells, but in contrast, U2OS cells show enhanced viability at high toxin concentrations if PJ-34 is added.

8. Discussion

8.1. Comparison of Lysis Protocols

To isolate functional PARP1 from human cells as complete as possible, five lysis protocols were compared: LPSC, CHAPS, RIPA as well as modified versions of CHAPS and RIPA, adapted from their original protocols. The resulting protocol should be as easy and fast as possible, with extraction of entire PARP1 also from chromatin-bound state and maintaining its activity. Genomic DNA-free lysates would be preferable but not mandatory as other published protocols use permeabilized cells.

Table 8 gives an overview of the performance of the different lysis protocols. The three methods resulted in unequal total protein yields (Table 6), although the identical starting material and lysis buffer volume was used.. The differences are probably due to differences in lysis-quality and associated protein loss during the two centrifugation steps. However, regardless of protein–PARP1 ratio, total PARP1 yield was of major concern and was highest for LPSC. Additionally, isolates by LPSC lacked genomic DNA in final lysate after Protamine sulfate treatment. Finally, best preservation of enzymatic activity was achieved also by LPSC and so it was selected as lysis protocol of choice for further evaluation.

	LPSC	CHAPS	CHAPS mod.	RIPA	RIPA mod.
PARP1 Amount	+	-	(+)	/	(+)
DNA Extraction	+	/	+	-	-
PARP1 Aktivity	+	/	(+)	/	-

Table 8: Summary of lysis protocol comparison. (-) unsatisfying result, ((+)) fair result, (+) good result, (/) not tested

8.2. Modifications of LPSC Protocol

After having chosen LPSC as standard protocol for cell lyses, protocol modifications were made for optimization.

8.2.1. PAR Stability During Lysis

PAR stability / integrity during the process of lysing is indispensable not only in terms of PAR forming in-cell treatments prior to lysis but also for activity assays with extracted PARP, which are based upon preservation of preformed PAR.

PARP1 activity is composed of total PARP1 amount, allele present in the cell and level of pre-modification. Modified PARP1 has lower activity, making basal auto-modification an important aspect for the assays (Kawaichi et al., 1981). On Western blot membrane, PARylated PARP1 was detectable for untreated as well as H_2O_2 treated cells. As expected, the PARP inhibitor PJ-34 prevented PAR formation (PJ-34 and PJ-34/ H_2O_2). PAR in untreated cells demonstrated constitutive low PARP activity. Higher PAR levels in 1 mM H_2O_2 treated samples corresponded to activation of PARP.

Drop in PAR level in supernatants 2 indicated loss of auto-modified PARP1 during Protamine sulfate precipitation, probably due to the nucleic acid-like

nature of PAR. Thus, Protamine sulfate did not only free the samples of DNA, but also of PAR. Since pre-modification is an important aspect in determination of cellular capacity of PARP activity, Protamine sulfate had to be replaced.

8.2.2. Protamine Sulfate versus DNase I

To prevent loss of auto-modified PARP1 during lysing process, but still eliminate genomic DNA, trials were carried out with DNase I. Different concentrations were added to supernatant 1 from LPSC lysate and tested for disappearance of DNA.

Addition of DNase I led to a dose-dependent, yet incomplete DNA digestion. When testing for PARP1 integrity after DNase I incubation all but one sample revealed PARP1 cleavage. Thus, purification of samples from DNA could not be achieved with easy to handle methodology. However, as PARP activity assays using permeabilized cells also contain genomic DNA, this may not be of major concern, as in these protocols PARP activity was significantly induced above background by activator oligonucleotide (Grube et al., 1991; Zaremba et al., 2009).

8.2.3. Dialysis versus Filtration

For additional protocol shortening, the dialysis step for activity assay samples was tentatively replaced by filtration. Samples neither dialyzed nor filtered served as control.

In direct comparison, dialysis demonstrated higher PARP activity than filtration or control. This may be explained by the character of dialysis, diffusing out all smaller molecules like detergents (NP40, Tween 20) which are responsible for affecting PARP1 in activity. Filtration was either unsuccessful in removing disruptive agents or lower activity was due to PARP1 loss into the filter. However, dialysis is the major time-consuming step in the protocol, not permitting the assays to be completed within one day. Signal intensity of control was weaker but evaluable and sufficient to compare cell lines to one another. Consequently, it was decided to use samples from supernatant 1 without any further treatment.

8.2.4. TCA versus PBS

So far, basic PAR was hardly ever detected on slot blot membranes, whereas PAR in standard Western blotting using larger input volumes could be readily detected. However, pre-modified PARP1 is one important aspect of basic PARP activity and needed to be included in the assays. Replacing TCA was an attempt in this direction.

When reactions were stopped with PJ-34, with subsequent dilutions and membrane washed in PBS instead of stopping with 1 volume 20 % TCA and dilutions and washes with 10 % TCA, respectively, signal strength of samples on membranes could be intensified. Moreover, with longer development times, preformed PAR became visible for PJ-34/ PBS samples only.

The possibility of continuous PAR formation despite PJ-34 addition and during dilution in PBS was excluded by stopping reactions first with PJ-34 and

subsequently with liquid nitrogen before PBS dilution. Without glycerol in samples to protect proteins from crystallizing, freezing and thawing would alter enzyme functions and prevent further PAR formation and degradation. Nonetheless, samples again displayed stronger signals according to first experiments (data not shown). Therefore, TCA seemed to be responsible for signal weakening. TCA denatures proteins in the sample and apparently masks PAR from antibody.

8.2.5. Final LPSC Protocols

All reaction times for activity assays from 30 seconds to 3 minutes led to proportionate PAR formation. Standard time was defined as one minute, as this yielded reasonable amounts of PAR.

After some modifications, final protocol for activity assay was set as follows:

Lysis of cell pellet with LPSC buffer, 20 minute incubation at 4 °C and centrifugation at 16,100 x g for 20 minutes at 4 °C before sample was mixed with two volumes 30 % glycerol / PBS (to end concentration of 20 %). PAR forming reactions of one minute were stopped by one volume PJ-34 / PBS (10 µM end concentration) samples were diluted in PBS for application and slot washes were also performed with PBS.

For treatment of intact cells, the basic protocol was further shortened to avoid degradation of synthesized PAR by PARG and repress process-induced PARylation: for cell treatments prior to lysis, two modified protocols were tested. The first included incubation and one centrifugation step. Results showed PJ-34 treated samples completely lacking PAR due to inhibition of PARP1. Strong PAR signals were visible for control sample and slight signals for H_2O_2 treatment. This was unexpected, as H_2O_2 challenge of cells leads to higher PAR formation than untreated controls. However, it seems that PAR from H_2O_2 sample was degraded during the prolonged lysis step as damage induced PAR has a short half-life. The control sample displays the basal PAR level. As constitutive PAR is not as sensitive for degradation as PAR formed in consequence of DNA damage, PAR in control sample persisted through lysis steps, whereas the other was degraded.

The second, further improved protocol demonstrated the expected results. Leaving out incubation and centrifugation steps, PAR integrity was maintained and PAR intensity was stronger for treated sample. Final protocol consisted of cell treatment, reaction stop by freezing, 2x lysis buffer addition, PBS dilution and loading.

8.3. Activity Assays and PARP1 Amount

After having established a suitable cell lysis protocol and standard activity assay conditions, different cancer cell lines were analyzed for enzyme kinetics, PARP1 pre-modification, level of PAR production and PARP1 amount.

Since in these experiments PAR production was determined from cell lysates instead of recombinant PARP1, it cannot be excluded that any other PARP is contributing to total PAR levels. However, only six members of the family are true polymerases and thus only their activity can be detected by the used antibody. In addition, only PARP1, PARP2 and – to a much lesser extent – PARP3 can be activated by DNA strand breaks. Finally, up to 90 % of PAR formed upon

DNA damage (Shieh et al., 1998) stems from PARP1. Thus, the majority of detected PAR is synthesized by PARP1.

As presented in Figure 13, PARP activity in all cell lines displayed similar Michaelis-Menten kinetics. At low NAD^+ concentrations curves followed a sigmoidal shape typical for dimerization-based activity of PARP1. Increasing NAD^+ yields productive protein dimerization and PAR-synthesis is in a linear range. At higher concentrations, PAR-synthesis cannot be increased anymore and reaches a plateau due to saturating conditions. In addition, PARPs inactivate themselves by automodification, thus reducing their activity with every new ADP-ribose unit attached.

Based on an in parallel applied PAR-standard with known concentration, enzyme parameters can be calculated from the Michaelis-Menten kinetics. While K_M values were not different between the human cell lines, V_{max} values displayed significant variations (see Table 7).

All cell lines already displayed PAR signals in control samples. As no NAD^+ is added to these reactions, this indicates constitutive, basic PAR levels. Basal PAR was shown to have a by far longer half time than PAR formed upon DNA damage (hours versus seconds; Alvarez-Gonzalez & Althaus, 1989). Constitutive PAR in this study ranged from 1.7 pmol / 10^6 cells for HeLa to 48 pmol / 10^6 cells for MCF-7, compared to 132 pmol / 10^6 cells for peripheral blood lymphocytes measured by Plummer et al. (2005).

MCF-7 also showed the highest total PAR production with 1054 pmol/ 10^6 cells as opposed to HepG2 with only 505 pmol/ 10^6 cells, measured from the basal PAR level. Similar but higher results were demonstrated by Zaremba et al. (2009), who also showed a wide variation in PARP activities of different cancer cells. Surprisingly MCF-7 cells demonstrated the highest basal PAR level and concurrently highest PARP activity, even though pre-modification is reducing PARP activity (Kawaichi et al., 1981).

When testing for PARP1 amount, the cancer cell lines showed distinct variation with HeLa having over 6 times more PARP1 than U2OS cells. This is comparable to Zaremba et al. (2009), who found a range in PARP1 levels varying by factor 3.5 in tested human cancer cell lines. Significant differences were seen for some cell lines (Fig. 14). HeLa cells presented the highest PARP1 amount with 178 ng / 10^6 cells and U2OS the least with 28 ng /10^6 cells (Table 9). Possible correlations of PARP1 amount to cell size can be excluded since HeLa cells displayed a twofold higher PARP1 level than MCF-7 cells, despite the bigger size of MCF-7 cells (16 µm compared to 13 µm for HeLa; bionumbers.hms.harvard.edu/). SH-SY5Y on the other hand demonstrated a four times lower PARP1 amount than HeLa with a cell size only marginally smaller (12 µm). In Ewing sarcoma cells the exceptionally high PARP1 levels were found to be the result of transcriptional control (Soldatenkov et al., 1999).

Additionally, PARP1 levels, PAR production and basal PAR did not correspond (Table 9). Considering the two cell lines forming the most PAR, MCF-7 and HeLa indeed had the highest PARP1 amounts, yet basal PAR levels were opposing. MCF-7 cells were shown to have the highest pre-modification combined with maximum PAR formation, even though pre-modified PARP1 was found to have a reduced activity (Kawaichi et al., 1981). However, on closer observation all kinds of combinations could be seen. Zaremba et al. (2009) showed similar results.

However, while in their study MCF-7 cells were only classified in medium range of PARP activity, here they demonstrated highest PAR production.

for 10^6 cells	PARP1 level	max. PAR formation	basal PAR
HeLa	178 ng	1045 pmol	1.7 pmol
HepG2	78 ng	504 pmol	43 pmol
MCF-7	88 ng	1054 pmol	48 pmol
SH-SY5Y	43 ng	642 pmol	2.6 pmol
U2OS	28 ng	716 pmol	17 pmol

Table 9: Summary of cells in three different categories, from lowest (dark red) over mid-ranking (white) to highest (dark green) results. Statistical significance was not considered.

Yet, several aspects for activity would still have to be considered, such as allele present in cell as well as protein composition. In cells with high levels of acceptor proteins, PARP1 can transfer PAR onto other proteins and remains active, thus explaining differences in cell lines. However, even in the same cell line basal PAR levels and PARP activity do not always seem to correlate: Martello et al. (2013) tested human lymphocytes and found little difference in constitutive PAR levels. However, PAR formation in the cells varied highly after H_2O_2 challenge in between donors from a minimum of 20 fold to a maximum of 300 fold increased PAR synthesis.

8.4. H_2O_2 Treatment of Cells

After performing activity assays and measuring maximum PAR amounts produced under ideal conditions, PAR forming capacity in intact cells was to be determined by challenging cells with different H_2O_2 concentrations.

In these trials, all cell lines showed a wide variation in constitutive PAR level, not consistent with basic PAR levels in the activity assays. In general, constitutive PAR levels in H_2O_2 treatments were equally high or higher than PAR levels in first sample (0 mM H_2O_2). While controls for basal PAR were frozen directly, all other samples were treated at 37 °C for 5 minutes (pre-incubation and reaction time). During this period, still active poly(ADP-ribose)glycohydrolase in the samples could have degraded present PAR, leading to signal loss.

H_2O_2 treatments of intact cells presented lower PAR production than activity assays with lysates (2 pmol versus 1045 pmol for HeLa). In both cases PARP was intentionally activated and while dsDNA was used in activity assays, H_2O_2 was applied for cell treatments. Nevertheless, amount of DNA breaks induced by H_2O_2 is low compared to activation by dsDNA. Moreover, H_2O_2 can also cause damage to proteins, thus reducing PARP activity furthermore. Additionally, in cell treatments no substrate was added compared to activity assays. Therefore NAD^+ constituted the limiting factor for the reaction and degree of PAR formation was defined by available NAD^+ in cells. Nonetheless, course of curve did not change and sigmoidal shape was still implied for most cell lines. Again, lowest PAR formation was measured for HepG2 and highest for MCF-7.

8.5. PARP Inhibitor and H_2O_2 Treatment of Cells

H_2O_2 trials were followed by H_2O_2/ PJ-34 combined treatments. Performing PARP1 inhibitor concentration trials allows the determination of the PARP1 plasticity, thus facilitating individual cancer therapies and making a step towards personalized medicine.

In PJ-34 treatments only HepG2 cells showed different results for low and high H_2O_2. In the other cell lines PJ-34 was equally effective in abrogating PARP activity for both H_2O_2 concentrations. As soon as PJ-34 level in cells fully block PARP activity, PAR formation is stopped, regardless of how high DNA damage is at that point. Some cell lines seemed to be more sensitive to PJ-34 inhibition than others. When looking at the decrease in PAR production in percent from the control, all cell lines except HeLa cells showed a distinct reduction already after the first PJ-34 addition. However, at higher concentrations differences in the plasticity of the cancer cell lines were manifested and while for some cell lines low PJ-34 concentrations were sufficient, PAR formation in others was not even completely blocked at the highest used PJ-34 dosages. In SH-SY5Y cells PAR production was abrogated already at lowest PJ-34 concentration. As SH-SY5Y cells demonstrated lower PAR production upon challenge, probably also low PJ-34 concentrations are able to fully inhibit PARP. Yet this is not detected in all cell lines. HeLa cells showed high PAR formation in previous experiments, but was also inhibited by PJ-34. In contrast, MCF-7 and U2OS PAR synthesis were only partially reduced even at highest PJ-34. Experiments with higher inhibitor dosages will have to be conducted for these cell lines.

8.6. Viability Assays

Effects of H_2O_2 and temozolomide on viability were tested in the five cancer cell lines. Treating them with two different cytotoxic agents demonstrated dependence of sensitivity on respective cell lines and agents.

Challenged with H_2O_2 HeLa, HepG2 and U2OS cells showed similar reactions in the assays with HepG2 differing particularly in a higher final viability at maximum toxicity. This representing the midfield, the two remaining cell lines SH-SY5Y and MCF-7 covered the extremes: while SH-SY5Y cells were highly sensitive to H_2O_2 treatment with distinct reduction in viability already at very low concentrations, MCF-7 cells were barely affected.

However, this changed in temozolomide assays and MCF-7 viability was impaired to a higher extend, whereas SH-SY5Y was affected less. HeLa, HepG2 and U2OS cells reacted similar to H_2O_2 challenges.

PARP1 inhibitor influence likewise varied with cell line and PJ-34 effect was not solely protective but depended on concentration of H_2O_2 and temozolomide. Seen in all cell lines to a small extend, in SH-SY5Y cells a biphasic effect of PJ-34 was clearly observed. At lower toxic concentrations PJ-34 treated cells were slightly less viable than those having received cytotoxic treatment alone. Combination of DNA damaging agents and impairment of DNA single strand repair by PARP inhibitor leads to strong accumulation of double strand breaks, thus overstraining HR (He et al., 2010) and eventually causing cell death. Low DNA damage by small concentrations of cytotoxic agents only moderately activates PARP1 to induce DNA repair. In this scenario, HR is able to compensate the inhibition of PARP1 and repair occurring DNA double strand breaks.

However, PJ-34 inhibition blocks PARP1 enzymes at DNA damage sites and disturbs repair (Murai et al., 2012). Consequently, cells are driven into apoptosis. At higher toxic concentrations PJ-34 acted protective in all cell lines, except MCF-7 and SH-SY5Y when treated with H_2O_2. A high burden in DNA breaks massively induces PARP activity, leading to a severe drop in NAD^+ levels. In an attempt to re-synthesize this important redox-molecule, ATP is salvaged and the cell subsequently succumbs to energy loss (Zong et al., 2004). Abrogating PARP activity at these concentrations of cytotoxins is beneficial as it prevents NAD^+ depletion.

9. Conclusion

Five human cancer cell lines were compared in aspects of PARP1 amount, PARP activity, basic and damage-induced PAR levels, PARP1 inhibitor concentrations as well as cytotoxic sensitivity. As different as these cell lines are, so were their results.

Regarding PARP1 none of the above mentioned aspects seemed to correlate: high PARP1 amount in cells with little pre-modification did not entail high PAR production upon challenge. Instead, all possible combinations were seen, emphasizing just how little is understood so far about the enzyme. According to these results, Zaremba et al. (2009) neither found a correlation between PARP1 amount and activity nor between PARP1 amount and polymorphism. Another study (Martello et al., 2013) measured PARP1 amount in different mouse tissue: organs with mediocre PARP1 level showed high basal PAR, whereas those with high PARP1 showed low basal PAR, thus suggesting another context of PARP1 level and constitutive PAR.

Cell viability after cytotoxic treatments varied with cell lines and cytotoxic agents. While cells are sensitive to one agent another one is less effective. For cancer therapy this would mean that extrapolating from one chemotherapeutic drug to another might result in loss of efficacy. Even cancer subtypes show different reaction patterns, as Hastak et al. (2010) demonstrated with breast cancer: while cells of the basal-like subtype increasingly go into apoptosis when treated with an agent, the luminal breast cancer subtype might not be impaired or even give contrasting results. Individual treatments have to be conducted and drug sensitivity determined for each type of cancer. When sensitivity is confirmed, choosing the right inhibitor concentration might still be challenging. Due to the biphasic curve course it is crucial to determine the transition from negative to protective inhibitor effect. Trapping degree of PARP1 on DNA by PARP inhibitors also varies with the applied inhibitor (Murai et al., 2012).

All these different parameters make it necessary in therapy to measure PARP activity, define sensitivity and investigate inhibitor concentrations for each cell type, thus ensuring individual treatments.

10. Outlook

The next logical step is performing the cell treatments done here in this work with H_2O_2 in detail with different chemotherapeutic drugs before switching to an in vivo model. Tumors formed by cancer cell lines engrafted into mice would be the model of choice. Cells can be re-isolated from tumor masses and compared to the parental cells regarding activity and other parameters. For this, a new protocol for the isolation of the cells from cancer mass has to be established. In addition, impact of stroma cells within the tumor on measured values can be monitored, as the ratio of human cancer to normal mouse cells can be determined. Results from this approach can then be used to extend the study to human cancer biopsies. A fully validated protocol emerging from these experiments would be a step towards personalized cancer therapy, now taking into account differences in PARP activity, plasticity (sensitivity to inhibitor) as well as general responsiveness to the respective cytotoxin applied.

It should be of major concern to use inhibitors which selectively target only PARP1. Since many functions of the different PARP family members are still unknown, side effects cannot be estimated to the full extent, especially when inhibitors are administered in long term.

Drug interactions also need to be taken into account, particularly in matters of toxic concentrations. Sensitivity for certain drugs is influenced depending on which PARP enzyme is knocked out in a cell: e.g. PARP1 or PARP2 negative cells vary in rendering cells more receptive to different chemotherapeutics (Hastak et al., 2010).

As PARP1 plays many roles in cell homeostasis, overall goal must be to inhibit PAR production only so much, that basal PARP1 activity of normal cells stays unaffected. Effects of chemotherapeutic drugs can be enhanced by combination with PARP1 inhibitors, consequently allowing dose reductions and minimizing side effects. Treatments should be chosen according to individual needs, thus improving personalized medicine.

11. References

Alvarez-Gonzalez, R., & Althaus, F. R. (1989). Poly (ADP-ribose) catabolism in mammalian cells exposed to DNA-damaging agents. *Mutation Research/DNA Repair*, *218*(2), 67-74.

Alvarez-Gonzalez, R., & Mendoza-Alvarez, H. (1995). Dissection of ADP-ribose polymer synthesis into individual steps of initiation, elongation, and branching. *Biochimie*, *77*(6), 403-407.

Beneke, S., Alvarez-Gonzalez, R., & Bürkle, A. (2000). Comparative characterisation of poly (ADP-ribose) polymerase-1 from two mammalian species with different life span. *Experimental gerontology*, *35*(8), 989-1002.

Beneke, S., Diefenbach, J., & Bürkle, A. (2004). Poly (ADP-ribosyl) ation inhibitors: promising drug candidates for a wide variety of pathophysiologic conditions. *International journal of cancer*, *111*(6), 813-818.

Beneke, S., Cohausz, O., Malanga, M., Boukamp, P., Althaus, F., & Bürkle, A. (2008). Rapid regulation of telomere length is mediated by poly (ADP-ribose) polymerase-1. *Nucleic acids research*, *36*(19), 6309-6317.

Beneke, S., Scherr, A. L., Ponath, V., Popp, O., & Bürkle, A. (2010). Enzyme characteristics of recombinant poly (ADP-ribose) polymerases-1 of rat and human origin mirror the correlation between cellular poly (ADP-ribosyl) ation capacity and species-specific life span. *Mechanisms of ageing and development*, *131*(5), 366-369.

Bürkle, A. (2001). Physiology and pathophysiology of poly (ADP-ribosyl) ation. *Bioessays*, *23*(9), 795-806.

Cepeda, V., Fuertes, M. A., Castilla, J., Alonso, C., Quevedo, C., Soto, M., & Pérez, J. M. (2006). Poly (ADP-ribose) polymerase-1 (PARP-1) inhibitors in cancer chemotherapy. *Recent patents on anti-cancer drug discovery*, *1*(1), 39-53.

Chiang, F. Y., Wu, C. W., Hsiao, P. J., Kuo, W. R., Lee, K. W., Lin, J. C., Liao, Y.C., & Juo, S. H. H. (2008). Association between polymorphisms in DNA base excision repair genes XRCC1, APE1, and ADPRT and differentiated thyroid carcinoma. *Clinical Cancer Research*, *14*(18), 5919-5924.

Delaney, C. A., Wang, L. Z., Kyle, S., White, A. W., Calvert, A. H., Curtin, N. J., Durkacz, B. W., Hostomsky, Z., & Newell, D. R. (2000). Potentiation of temozolomide and topotecan growth inhibition and cytotoxicity by novel poly (adenosine diphosphoribose) polymerase inhibitors in a panel of human tumor cell lines. *Clinical cancer research*, *6*(7), 2860-2867.

Diefenbach, J., & Bürkle, A. (2005). Introduction to poly (ADP-ribose) metabolism. *Cellular and molecular life sciences: CMLS*, *62*(7-8), 721-730.

Ekblad, T., Camaioni, E., Schüler, H., & Macchiarulo, A. (2013). PARP inhibitors: polypharmacology versus selective inhibition. *FEBS Journal*, *280*(15), 3563-3575.

El-Khamisy, S. F., Masutani, M., Suzuki, H., & Caldecott, K. W. (2003). A requirement for PARP-1 for the assembly or stability of XRCC1 nuclear foci at sites of oxidative DNA damage. *Nucleic acids research*, *31*(19), 5526-5533.

Fahrer, J., Kranaster, R., Altmeyer, M., Marx, A., & Bürkle, A. (2007). Quantitative analysis of the binding affinity of poly (ADP-ribose) to specific binding proteins as a function of chain length. *Nucleic acids research*, *35*(21), e143-e143.

Figueroa, J. D., Malats, N., Real, F. X., Silverman, D., Kogevinas, M., Chanock, S., Welch, R., Dosemeci, M., Tardón, A., Serra, C., Carrato, A., García-Closas, R., Castaño-Vinyals, G., Rothman, N., & García-Closas, M. (2007). Genetic variation in the base excision repair pathway and bladder cancer risk. *Human genetics*, *121*(2), 233-242.

Fiorillo, C., Ponziani, V., Giannini, L., Cecchi, C., Celli, A., Nassi, N., Lanzilao, L., Caporale R., & Nassi, P. (2006). Protective effects of the PARP-1 inhibitor PJ34 in hypoxic-reoxygenated cardiomyoblasts. *Cellular and Molecular Life Sciences CMLS*, *63*(24), 3061-3071.

Flohr, C., Bürkle, A., Radicella, J. P., & Epe, B. (2003). Poly (ADP-ribosyl) ation accelerates DNA repair in a pathway dependent on Cockayne syndrome B protein. *Nucleic acids research*, *31*(18), 5332-5337.

Gangopadhyay, N. N., Luketich, J. D., Opest, A., Visus, C., Meyer, E. M., Landreneau, R., & Schuchert, M. J. (2011). Inhibition of poly (ADP-ribose) polymerase (PARP) induces apoptosis in lung cancer cell lines. *Cancer investigation*, *29*(9), 608-616.

Gao, R., Price, D. K., Sissung, T., Reed, E., & Figg, W. D. (2008). Ethnic disparities in Americans of European descent versus Americans of African descent related to polymorphic ERCC1, ERCC2, XRCC1, and PARP1. *Molecular cancer therapeutics*, *7*(5), 1246-1250.

Gibson, B. A., & Kraus, W. L. (2012). New insights into the molecular and cellular functions of poly (ADP-ribose) and PARPs. *Nature reviews Molecular cell biology*, *13*(7), 411-424.

Grube, K., Küpper, J. H., & Bürkle, A. (1991). Direct stimulation of poly (ADP ribose) polymerase in permeabilized cells by double-stranded DNA oligomers. *Analytical biochemistry*, *193*(2), 236-239.

Grube, K., & Bürkle, A. (1992). Poly (ADP-ribose) polymerase activity in mononuclear leukocytes of 13 mammalian species correlates with species-specific life span. *Proceedings of the National Academy of Sciences*, *89*(24), 11759-11763.

Haince, J. F., Kozlov, S., Dawson, V. L., Dawson, T. M., Hendzel, M. J., Lavin, M. F., & Poirier, G. G. (2007). Ataxia telangiectasia mutated (ATM) signaling network is modulated by a novel poly (ADP-ribose)-dependent pathway in the early response to DNA-damaging agents. Journal of Biological Chemistry, 282(22), 16441-16453.

Haince, J. F., McDonald, D., Rodrigue, A., Déry, U., Masson, J. Y., Hendzel, M. J., & Poirier, G. G. (2008). PARP1-dependent kinetics of recruitment of MRE11 and NBS1 proteins to multiple DNA damage sites. Journal of Biological Chemistry, 283(2), 1197-1208.

Hastak, K., Alli, E., & Ford, J. M. (2010). Synergistic chemosensitivity of triple-negative breast cancer cell lines to poly (ADP-Ribose) polymerase inhibition, gemcitabine, and cisplatin. *Cancer research*, *70*(20), 7970-7980.

He, J. X., Yang, C. H., & Miao, Z. H. (2010). Poly (ADP-ribose) polymerase inhibitors as promising cancer therapeutics. *Acta Pharmacologica Sinica*, *31*(9), 1172-1180.

Hottiger, M. O., Hassa, P. O., Lüscher, B., Schüler, H., & Koch-Nolte, F. (2010). Toward a unified nomenclature for mammalian ADP-ribosyltransferases. *Trends in biochemical sciences*, *35*(4), 208-219.

Huang, S. H., Xiong, M., Chen, X. P., Xiao, Z. Y., Zhao, Y. F., & Huang, Z. Y. (2008). PJ34, an inhibitor of PARP-1, suppresses cell growth and enhances the suppressive effects of cisplatin in liver cancer cells. *Oncology reports*, *20*(3), 567-572.

Ji, Y., & Tulin, A. V. (2010). The roles of PARP1 in gene control and cell differentiation. *Current opinion in genetics & development*, *20*(5), 512-518.

Kawaichi, M., Ueda, K., & Hayaishi, O. (1981). Multiple autopoly (ADP-ribosyl) ation of rat liver poly (ADP-ribose) synthetase. Mode of modification and properties of automodified synthetase. *Journal of Biological Chemistry*, *256*(18), 9483-9489.

Kawamitsu, H., Hoshino, H., Okada, H., Miwa, M., Momoi, H., & Sugimura, T. (1984). Monoclonal antibodies to poly (adenosine diphosphate ribose) recognize different structures. *Biochemistry*, *23*(16), 3771-3777.

Krukenberg, K. A., Jiang, R., Steen, J. A., & Mitchison, T. J. (2014). Basal Activity of a PARP1-NuA4 Complex Varies Dramatically across Cancer Cell Lines. Cell reports.

Lockett, K. L., Hall, M. C., Xu, J., Zheng, S. L., Berwick, M., Chuang, S. C., Clark, P. E., Cramer, S. D., Lohman, K., & Hu, J. J. (2004). The ADPRT V762A genetic variant contributes to prostate cancer susceptibility and deficient enzyme function. *Cancer research*, *64*(17), 6344-6348.

Mangerich, A., & Bürkle, A. (2011). How to kill tumor cells with inhibitors of poly (ADP-ribosyl) ation. *International journal of cancer*, *128*(2), 251-265.

Martello, R., Mangerich, A., Sass, S., Dedon, P. C., & Bürkle, A. (2013). Quantification of Cellular Poly (ADP-ribosyl) ation by Stable Isotope Dilution Mass Spectrometry Reveals Tissue-and Drug-Dependent Stress Response Dynamics. *ACS chemical biology*, *8*(7), 1567-1575.

Murai, J., Shar-yin, N. H., Das, B. B., Renaud, A., Zhang, Y., Doroshow, J. H., Ji, J., Takeda, S., & Pommier, Y. (2012). Trapping of PARP1 and PARP2 by clinical PARP inhibitors. *Cancer research*, *72*(21), 5588-5599.

Plummer, E. R., Middleton, M. R., Jones, C., Olsen, A., Hickson, I., McHugh, P., Margison, G. P., McGown, G., Thorncroft, M., Watson4, A. J., Boddy, A. V., Calvert, A. H., Harris, A. L., Newell, D. R., & Curtin, N. J. (2005). Temozolomide pharmacodynamics in patients with metastatic melanoma: DNA damage and activity of repair enzymes O6-alkylguanine alkyltransferase and poly (ADP-ribose) polymerase-1. *Clinical Cancer Research*, *11*(9), 3402-3409.

Plummer, R., Jones, C., Middleton, M., Wilson, R., Evans, J., Olsen, A., Curtin, N., Boddy, A., McHugh, P., Newell, D., Harris, A., Johnson, P., Steinfeldt, H., Dewji, R., Wang, D., Robson, L., & Calvert, H. (2008). Phase I study of the poly (ADP-ribose) polymerase inhibitor, AG014699, in combination with temozolomide in patients with advanced solid tumors. *Clinical Cancer Research*, *14*(23), 7917-7923.

Potaman, V. N., Shlyakhtenko, L. S., Oussatcheva, E. A., Lyubchenko, Y. L., & Soldatenkov, V. A. (2005). Specific binding of poly (ADP-ribose) polymerase-1 to cruciform hairpins. Journal of molecular biology, 348(3), 609-615.

Rouleau, M., Patel, A., Hendzel, M. J., Kaufmann, S. H., & Poirier, G. G. (2010). PARP inhibition: PARP1 and beyond. *Nature Reviews Cancer*, *10*(4), 293-301.

Ruscetti, T., Lehnert, B. E., Halbrook, J., Le Trong, H., Hoekstra, M. F., Chen, D. J., & Peterson, S. R. (1998). Stimulation of the DNA-dependent protein kinase by poly (ADP-ribose) polymerase. Journal of Biological Chemistry, 273(23), 14461-14467.

Shieh, W. M., Amé, J. C., Wilson, M. V., Wang, Z. Q., Koh, D. W., Jacobson, M. K., & Jacobson, E. L. (1998). Poly (ADP-ribose) polymerase null mouse cells synthesize ADP-ribose polymers. *Journal of Biological Chemistry*, *273*(46), 30069-30072.

Shiobara, M., Miyazaki, M., Ito, H., Togawa, A., Nakajima, N., Nomura, F., Morinaga, N., & Noda, M. (2001). Enhanced polyadenosine diphosphate-ribosylation in cirrhotic liver and carcinoma tissues in patients with hepatocellular carcinoma. *Journal of gastroenterology and hepatology*, *16*(3), 338-344.

Smith, S. (2001). The world according to PARP. *Trends in biochemical sciences*, *26*(3), 174-179.

Smith, T. R., Levine, E. A., Freimanis, R. I., Akman, S. A., Allen, G. O., Hoang, K. N., Liu-Mares, W., & Hu, J. J. (2008). Polygenic model of DNA repair genetic polymorphisms in human breast cancer risk. *Carcinogenesis*, *29*(11), 2132-2138.

Soldatenkov, V. A., Albor, A., Patel, B. K., Dreszer, R., Dritschilo, A., & Notario, V. (1999). Regulation of the human poly (ADP-ribose) polymerase promoter by the ETS transcription factor. *Oncogene*, *18*(27), 3954-3962.

Soriano, F. G., Virág, L., Jagtap, P., Szabó, É., Mabley, J. G., Liaudet, L., Marton, A., Hoyt, D. G., Murthy, K. G. K., Salzman, A. L., Southan, G. J., & Szabó, C. (2001). Diabetic endothelial dysfunction: the role of poly (ADP-ribose) polymerase activation. *Nature medicine*, *7*(1), 108-113.

Wang, X. G., Wang, Z. Q., Tong, W. M., & Shen, Y. (2007). PARP1 Val762Ala polymorphism reduces enzymatic activity. *Biochemical and biophysical research communications*, *354*(1), 122-126.

Whitaker, J. R., & Granum, P. E. (1980). An absolute method for protein determination based on difference in absorbance at 235 and 280 nm. *Analytical biochemistry*, *109*(1), 156-159.

Zaremba, T., Ketzer, P., Cole, M., Coulthard, S., Plummer, E. R., & Curtin, N. J. (2009). Poly (ADP-ribose) polymerase-1 polymorphisms, expression and activity in selected human tumour cell lines. *British journal of cancer*, *101*(2), 256-262.

Zaremba, T., Thomas, H. D., Cole, M., Coulthard, S. A., Plummer, E. R., & Curtin, N.J. (2011). Poly (ADP-ribose) polymerase-1 (PARP-1) pharmacogenetics, activity and expression analysis in cancer patients and healthy volunteers. *Biochemical Journal*, *436*(3), 671-679.

Zong, W. X., Ditsworth, D., Bauer, D. E., Wang, Z. Q., & Thompson, C. B. (2004). Alkylating DNA damage stimulates a regulated form of necrotic cell death. *Genes & development*, *18*(11), 1272-1282.

Acknowledgments

I would like to express my thanks to:

Prof. Dr. med. vet. Felix R. Althaus for giving me the opportunity to perform my doctoral thesis at the Institute of Veterinary Pharmacology and Toxicology.

PD Dr. rer. nat. Sascha Beneke for the thesis supervision, for ideas and suggestions, for always having the door open for trouble shooting and proofreading my dissertation.

PD Dr. med. vet. Carla Rohrer Bley for proofreading my dissertation.

Theresa Pesch for our chats, for listening, helping and always finding a solution for what-so-ever; “caffeine-containing hot beverage” -moments would not have been the same without you.

The other lab members: Chiara, Hans, Sandro, Tamara, Birgit, Zuzana, Marjo and Peter for entertaining lunch breaks, support and helpfulness. It was a pleasure sharing an office with you!

MSc Patricia Jaaks from the University Children's Hospital, Experimental Infectious Diseases and Cancer Research, Zürich) for the HepG2 cells.

Special thanks go to:

My family for always being there for me, for countless Skype-sessions and endless support and encouragement.

Mark Huwyler simply for everything, you are the best.

The Huwylers for becoming my Swiss family.

Curriculum Vitae

Vorname Name	Jennifer Brandenburg
Geburtsdatum	21.07.1987
Geburtsort	Tokio, Japan
Nationalität	Deutsch

Schulausbildung

1993 - 1994	Collegio Humboldt, Caracas, Venezuela
1994 - 1997	Grundschule, Meckenheim-Merl, Deutschland
1997 - 1998	Konrad Adenauer Gymnasium, Meckenheim, Deutschland
1998 - 2002	Eurocampus, Manila, Philippinen
2002 - 2006	German School, Washington D.C., USA

Höchster Schulabschluss

25/05/2006	Allgemeine Hochschulreife (Abitur)

Studium

09/2006 - 05/2007	Biologie, Universität Bern, Schweiz
09/2007 – 01/2013	Veterinärmedizin, Vetsuisse-Fakultät, Bern, Schweiz

Erhalt des Tierärzte-Diploms

23/01/2013	Vetsuisse-Fakultät, Bern, Schweiz

Anfertigung der Dissertation

04/2013 – 11/2014	unter Leitung von PD Dr. rer. nat. Sascha Beneke am Institut für Veterinärpharmakologie und Toxikologie der Vetsuisse-Fakultät Universität Zürich Direktor: Prof. Dr. med. vet. Felix R. Althaus